Norwegian University
of Life Sciences
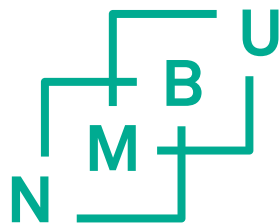
Vector corrections in scalar gravimetry

Magne Bugten

Geomatics
Faculty of Science and Technology

Norwegian University of Life Sciences
Faculty of Science and Technology

Vector corrections in scalar gravimetry

Magne Bugten

Norwegian University
of Life Sciences

Master's Thesis in
Geomatics

Norway
May 2018

Supervisors:
Bjørn Ragnvald Pettersen
Ove Christian Dahl Omang

Vector corrections
in scalar gravimetry

Magne Bugten

Abstract

Advances in airborne gravimetry have made increased use of global navigation satellite systems (GNSS) to successfully model unwanted accelerations, caused by the motion of the aircraft. Installation of GNSS receivers in ships carrying (traditional) sea gravimetry equipment enables the same kind of modelling for older systems. We wish to explore the use of GNSS derived accelerations in corrective models for a scalar sea gravimeter in pursuit of increased resolution and accuracy.

Unlike modern airborne (vector) gravimeters that are constructed with three perpendicular sensitive accelerometers, traditional sea gravimeters have only one sensitive axis to measure gravity with; this is why they are often referred to as 'scalar'. Traditional sea gravimeters orient their sensitive axis to the vertical using a gyrostabilized platform to maximise their sensitivity to the gravitational field. Like the airborne gravimeter, the sea gravimeters are also susceptible to noise from the movement of the ship, but, high-frequency horizontal accelerations are filtered out by the gyro stabilising platform.

Gravimetric and positional data was processed and analysed using Pandas DataFrames and SciPy signal analysis tools. Custom functions for signal conditioning and interpolation were employed to estimate the inertial state at the time of gravimetric readings. We present two methods using 3D and 1D acceleration derived from GNSS to correct measurements from a scalar gravimeter.

These methods, applied on two datasets, one real-time and one post-processed, are compared to a control method. The method using real-time generated data and 3D accelerations show good results, particularly in estimating and compensating for horizontal accelerations form situations outside the practical limitations of the stabilising platform. However, we have not obtained the crossover RMS performance of these methods.

Acknowledgements

Contents

List of Figures

Chapter 1

Introduction

A common saying among geodesists is that height systems become outdated the moment they are introduced. A height system defines a zero point to which heights can be measured. However, this creates a problem over time as, for instance in Norway, the entire country is slowly rising due to post-glacial rebound. It may not be much, but a few millimetres every year can amount to some significant differences. Thus, we are left with a problem: How to create a height system that accounts for post-glacial rebound?

One of the long-term goals of the Norwegian Mapping Authority (NMA) is to define a new height system using a well-defined geoid. Today, several companies and entrepreneurs in construction and surveying all over the country rely on accurate orthometric heights defined by the NN2000 height system. These heights can be related to the ellipsoid using the HREF model that the NMA distributes. The HREF model enables anyone with adequate GNSS equipment to transfer ellipsoidal heights into the NN2000 reference frame. Without heights in NN2000, companies and entrepreneurs risk constructing on unlevel surfaces which can lead to mass miscalculation or even water flowing in the wrong direction through a pipe.

Unfortunately, HREF and the underlying geoid are poorly defined in coastal areas. Fjords that stretch far inland, and islands populating a highly fractal coastline contribute to a complex and undulating equipotential surface. To combat this problem, the NMA wants to use as much gravitational surveying data as possible to define a more accurate geoid. However, there exists an additional problem: There is no common frame of reference for land and sea surveying.

Because of this, the NMA launched an investigative survey in 2015 in an attempt to find means of relating the two reference frames. In a preliminary rapport of phase one of the survey by Bratheim (2017), one conclusion states that "[there is a need to improve the underlying data framework in coastal areas both at land and at sea]" in part referring to gravitational measurements.

Onboard MS Hyrdograf, a research vessel for the NMA sits a Bell instruments BGM-3 Sea gravimeter. In the period between November 2015 and September 2016, it continuously recorded gravimetric measurements at a rate of about 1 Hz. Wherever the ship sailed

in that period, there is potential to extract gravimetric data. However, the BGM-3 is quite old and has somewhat limited accuracy. Still, the NMA is interested in utilizing the BGM-3 to its fullest potential and wishes to explore whether additional GNSS information can increase resolution and accuracy.

1.1   Objective

The objective of this thesis is to investigate means of reducing the raw gravimetric data from the BGM-3 relative sea gravimeter into more accurate gravimetric observations using GNSS and to compare the results from the investigations with a previously established method. We implement the old method as a control, and we compare it to new methods using both real-time and a post-processed data. This may give the mapping authority a better foundation for its geoid model computations.

The focus of the investigations leans strongly toward the use of vectorised corrections, even though the BGM-3 is a scalar gravimeter. One motivation for this was the availability of 3D positioning data from the post-processing software TerraPos which uses a tightly coupled GNSS-INS solution. The other source of positional information, Kongsberg Seapath 330+, also uses a GNSS-IMU solution but provides real-time data in the form of NMEA sentences. Another motivation for considering vector corrections was the lack of an X-Y accelerometer in the BGM-3. To be clear, the BGM-3 has an X-Y accelerometer, but its readout is not accessible.

Chapter 2

Theoretical background

Measuring the gravitational field is somewhat of a multidisciplinary problem. First and foremost are the theoretical considerations from physical geodesy which instruct us to measure the Earths gravitational field, and strictly defines what the gravitational field is. Then there is the broad discipline of measuring physics, which limit what we can physically measure and introduces a host of interesting uncertainties. However, it all comes back to two very central mathematical descriptions of the physical world citepNewton1687:

$$F = ma \tag{2.1}$$

$$F = G\frac{m_1 m_2}{r^2} \tag{2.2}$$

2.1 Stokes and Koch

According to Hofmann-Wellenhof and Moritz (2006), Stokes formula (eq. 2.3) is the most important equation in physical geodesy. It can be described as such because it relates a measurable quantity, Δg, to the geoids height above the ellipsoid, N, which is increadibly important because it represents a realization of the Earths gravitational feild. However, Stokes formula still has its roots in Newton's law of universial gravity (eq. 2.2): They both provide a description of gravity. Stokes formula can be written as:

$$N = \frac{R}{4\pi\gamma_0} \iint\limits_{\sigma} \Delta g S(\psi) d\sigma \tag{2.3}$$

Where R is the Earth's radius, Δg is the gravity anomaly, and $S(\psi)$ represents Stokes *function*. For this thesis, stokes function can be described as a weighting function that determines the contribution of Δg based on the ellipsoidal distance ψ. Effectively, this
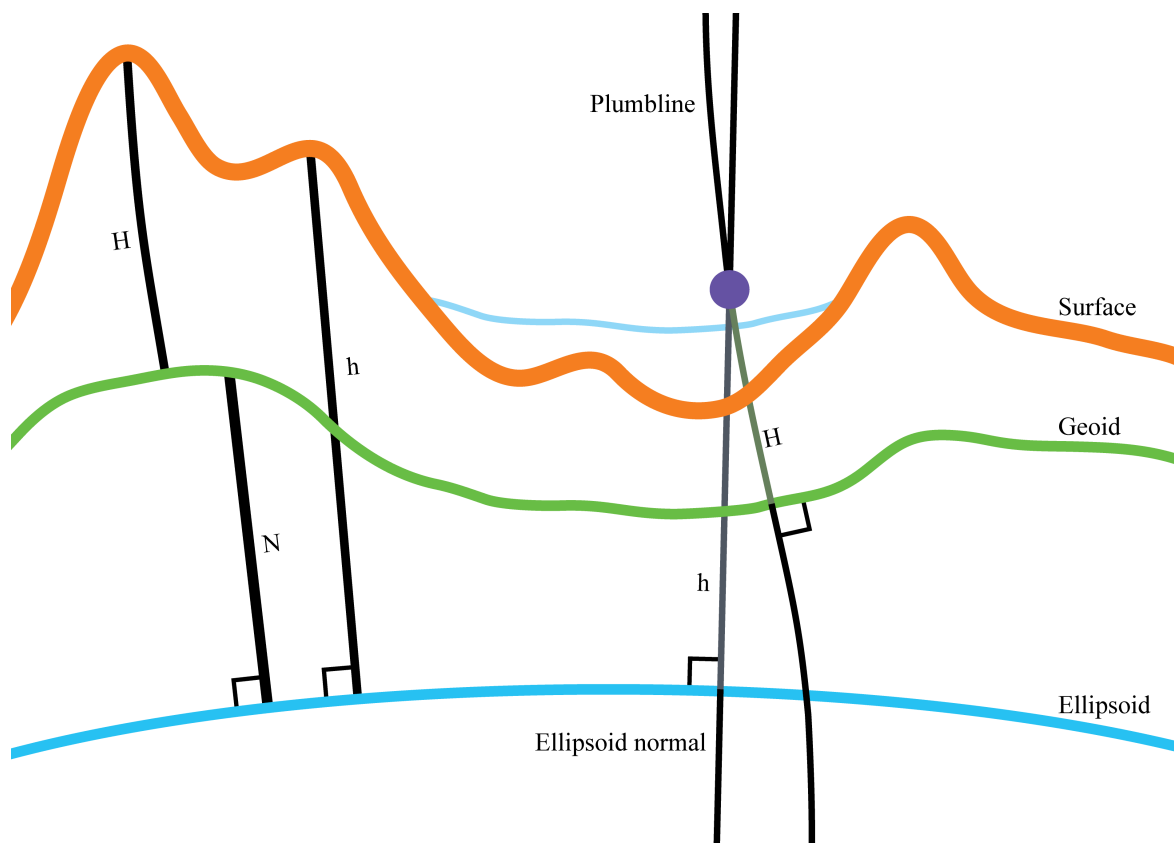
Figure 2.1: Relationships between the geoid, the ellipsoid and their relation to an arbitrary point above the surface. $h = N + H$

means that the local gravity anomaly, Δg, is essential when attempting to calculate the local geoid height (N). This serves to illustrate that the objective, ultimately for the mapping authority, is to determine geoid heights as a way to realise the gravitational field.

Koch's formula is not very different, but serves to relate another variable, gravity disturbance δg to the height of the geoid, N. Here, in Eq. 2.4 gravity disturbance takes the place of gravity anomaly, and the Hotine-Koch function, $K(\psi)$, takes the place of Stokes function (Hofmann-Wellenhof and Moritz, 2006). The essential difference in these two formulas is what they calculate N in reference to:

$$N = \frac{R}{4\pi\gamma_0} \iint\limits_{\sigma} \delta g K(\psi) d\sigma \qquad (2.4)$$

2.2 Anomalous gravity

As already stated, the purpose of this exercise is to acquire accurate gravimetric observations from the BGM-3 relative sea gravimeter. These gravimetric observations refer to
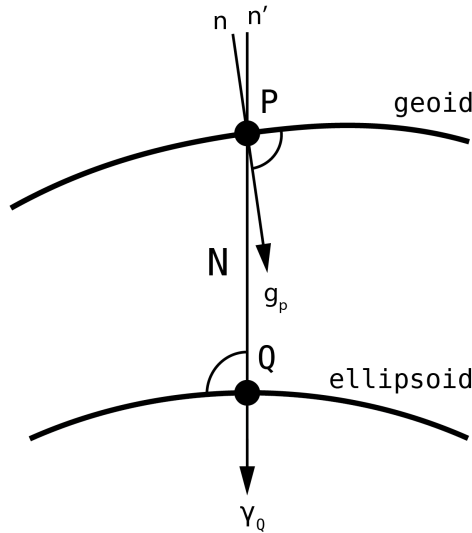
Figure 2.2: Geoid and reference ellipsoid

gravity anomaly, Δg, and gravity disturbance, δg. Gravity anomaly (eq. 2.5) is the difference between calculated gravity at a point on the ellipsoid (γ_Q) and the actual gravity at that same point projected on to the geoid (g_P). γ_Q and g_P will not only differ in terms of their scalar size due to the difference in height between the geoid and the ellipsoid but will also differ in direction by the deflection of the vertical. The deflection of the vertical is the angle between the ellipsoid normal, n' and the geoid normal n as depicted in figure 2.2.

$$\Delta g = g_P - \gamma_Q \tag{2.5}$$

Gravity anomaly is not to be confused with gravity disturbance, δg. Hofmann-Wellenhof and Moritz (2006) state that there is a possibility that δg may become more relevant in geodesy than Δg because point P is determined with GPS. By extension, gravity disturbances are used in the investigated methods because they employ GNSS in positioning (most importantly in relation to heights).

$$\delta g = g_P - \gamma_P \tag{2.6}$$

Where γ_P is the calculated gravitational contribution from the ellipsoid at the level of the geoid (projected from the ellipsoid). In practice, gravity is never measured on the geoid, and if it were, it would always yield the same measurement due to the equipotential nature of this theoretical surface. To obtain the gravity disturbance, for instance, it is necessary to project the measurement point from where it was made, down the plumb line to the geoid, and then make the calculation of theoretical gravity, γ_p, at the same location.

In practice, this is somewhat tedious due to the circular nature of this problem: Given

ellipsoidal height from GNSS at a point O, how do we project onto the geoid if we don't know where the geoid is. Therefore, we want to make a simplification: Let's say that $J()$ is the function that constitutes the additional gravity subtracted or added by an upwards or downwards continuation respectively (depending on the sign). We then apply this function such that $g_P = g_O - J(H)$ where H is the orthometric height above the geoid (that we don't know) and g_O is observed gravity at point O. By doing this, we have performed a downward continuation on the observed gravity g_O. Inserting this into equation 2.6, and rearranging yields:

$$\delta g = g_O - Y(H) - \gamma_P \tag{2.7}$$

$$\delta g = g_O - (\gamma_P + Y(H)) \tag{2.8}$$

In our case, g_O is always very close to the geoid, as we are measuring from a ship. Consider the relationship between the geoid and the ellipsoid from Figure 2.1, $h = N + H$, and let us make the simplification or assumption that:

$$\gamma_P + J(H) = \gamma_Q + J(h) \tag{2.9}$$

Theoretically, this consideration disregards the difference between the ellipsoid height of point O and height along the plumb line from the ellipsoid to point O. However, the difference is in practice very close to zero especially since we are measuring near the surface of the water. One way too look at this, is to consider the upward continuation of γ_Q by virtue of the height h, to yield the same result as an upward continuation of γ_P by virtue of H. Based on this we make the claim that we can use observed gravity and calculated gravity in point O to create gravity disturbances directly in the case of sea gravimetry. Moving forward, anomalous gravity will refer to both Δg and δg as if they are the same thing unless expressively stated otherwise.

$$\delta g = g_O - \gamma_O \tag{2.10}$$

2.3 Measuring gravity

Observing and measuring a gravitational field is complicated. Usually, a sensor measure the local acceleration and corrections must be made in order to estimate the value of the gravitational field. Einsteins equivalence principle (Einstein, 1915) tells us that inertial effects are impossible to distinguish from the effects of gravity.

The total acceleration measured by a stationary gravimeter is due to the gravity field (including tidal effects and the centrifugal effects from earth rotation), instrument drift, measuring uncertainties and local vibrations. Other signals that the gravimeter senses are most likely due to noise from the measurement electronics. To find the value of the

gravitational field, all other effects must be subtracted. This operation is often referred to as the observation equation and varies depending on the type of gravimeter and its attributes. However, if the gravimeter is situated on a moving platform the situation changes.

When measuring gravity from a moving platform, the gravimeter will also be subjected to the inertial effects of acceleration as the platform changes speed and direction. It will also be subjected to inertial effects from moving inside a rotating reference frame, known as Coriolis effects (Torge and Müller, 2012). Direct accelerations are easy to understand: Acceleration is the derivative of velocity with respect to time, and velocity is the derivative of position with respect to time. If the platform has any means of recording either its position or its velocity and direction, then these effects can be modelled and subtracted. Torge and Müller (2012) state: "The kinematic acceleration has to be determined independently by geometric methods of positioning and navigation, e.g., through GNSS". Torge and Müller then proceed to describe the gravity vector for a kinematic platform as:

$$g^l = \ddot{r}^l - R_b^l f^b + (2\Omega_{ie}^l + \Omega_{el}^l) \times \dot{r}^l \tag{2.11}$$

Where $\dot{r}^l$ the velocity represent, and $\ddot{r}^l$ the kinematic acceleration derived by GNSS by virtue of the second derivative of position with respect to time. f^b is the acceleration vector measured by the gravimeter in the platform body frame. The superscript l denotes a local reference frame. The third term describes the effects of movement in a non-inertial reference frame, i.e. the rotating earth. Note that the velocity, $\dot{r}^l$, is the observed size that controls the magnitude of the Coriolis effects. However, as Torge and Müller go on to explain, scalar gravimeters such as the BGM-3 sometimes only the sense the magnitude of the gravity vector. They collapse equation 2.11 to a scalar value:

$$g = f_Z - \ddot{Z} + 2\omega \cos\varphi \sin\alpha V + \frac{V^2}{r} \tag{2.12}$$

ω, φ, α, V and r are the angular velocity of Earths rotation, geodetic latitude, geodetic azimuth, platform velocity, and the distance from Earth centre, respectively. In this equation, everything relates to the local level vertical component. Meaning that these forces will be felt by a vertically oriented accelerometer. If the accelerometer fails to maintain verticality, observed gravity from the vertical will be reduced by the cosine of this deflection angle. This is supported and documented in the documentation for the stabilizing subsystem for the GBM-3 gravimeter (Bell, 1987): $g = g_{obs}\sin(\theta)$

2.3.1 Gravimeters

When measuring gravitational fields, the most accurate instruments are known as absolute gravimeters. These function by measuring the position of a test object (prism) dropped inside a vacuum chamber (typically around 20 cm in height). The position is recorded

carefully using an interferometer and timed by an atomic clock. Then the gravitational acceleration is calculated by the second derivative of position with respect to time. As can be surmised by this short description of their construction, absolute gravimeters are extremely sensitive and require a stable environment to operate in order not to pick up unwanted noise from vibrations or unwanted movement. Even so, absolute gravimeters require multiple measurements in order to obtain an accurate estimate of the gravitational situation they are in. Typically, their accuracy are on the order of 2 μGal.

The BGM-3 gravimeter described in section 3.2.1, is a relative gravimeter. Relative gravimeters work by measuring the force acting on a known test mass (eq. 2.1). They typically have an accuracy on the order of 1 - 5 mGal. Relative gravimeters can not sense the absolute strength of the gravitational field by themselves and require tie-points, points of known gravitation in space and time, in order to reliably provide gravimetric measurements. The most common relative gravimeters are Lacoste-Romberg gravimeters: They use a magnetic mass supported by a spring in an induced magnetic field. The spring is there to absorb most of the force, but the measurement comes from the amount of voltage used to generate the magnetic field that the test mass is partially suspended in. The BGM-3 works differently by levitating an electromagnet test mass inside a permanent magnetic field, and when changes in perceived acceleration change the position of the test mass, a feedback system applies the appropriate voltage to the electromagnet to stabilise the test mass inside the chamber.

2.3.2   Traditional sea gravimetry

To achieve good gravimetric measurements in the highly dynamic environment of the sea, purpose designed relative gravimeters, such as the BGM-3 must be used. Absolute gravimeters are not suited for this environment, with the possible exception of superconducting or quantum gravimeters. And common land-based relative gravimeters lack the accuracy or the supporting mechanisms to operate in such a dynamic environment. Typically, sea gravimeters measure gravity in the downward direction only (scalar gravimetry) because the sensitive axis of the instrument is oriented along the vertical by virtue of a stabilised platform (Bell, 1987), (Torge and Müller, 2012).

In traditional sea gravimetry, Δg is the desired variable to obtain. Therefore, in order to tie the relative gravimeter to an absolute value, a reading is performed at the same time for a point on the quay next to the ship[1] and simultaneously in the sea gravimeter. The level of the water at that time, relative to the quay, is also recorded. Since these measurements are taken together it is possible to disregard latitude corrections and tidal differences[2]. Since both points are stationary, no Eötvös or acceleration corrections are needed either. All that remains is to reduce the reference point down to the surface of the water (which could be viewed as the geoid itself) and set the sea gravimeter to equal that value.

---

[1]quay readings can be performed by an absolute gravimeter or by a different relative gravimeter that is already tied to a gravimetric network.

[2]There are none

In appendix B, the function *CV_adjustment* performs this tie-point adjustment while simultaneously translating the gravimeters readout from arbitrary *counter unit* values to accelerations in *mGal*. Relative gravimeters are also subject to drift, which must be corrected for. These items are discussed further when describing the BGM-3 in more detail in section 3.2.1.

2.3.3 Considerations from airborne gravimetry

In areal gravimetry, scalar gravimeters on stabilised platforms are used, but increasingly, vector gravimeters (strap-down INS gravimeters) are coming into use. In airborne gravimetry, the speeds are higher, and the accelerations are stronger than in sea gravimetry. We will use the 3D vector considerations often used in airborne gravimetry adapted to a traditional, scalar sea gravimeter.

Given that the navigation data from GNSS are sufficiently accurate, it is possible to reconstruct the inertial situation at the time of the gravimetric recordings. This should be done by calculating the accelerations, in three dimensions, for the lever arm point where the gravimeter is. To adapt this 3D acceleration vector to a scalar gravimeter, the vector must be collapsed to a value that represents the scalar contribution of these accelerations. This is done by appropriately filtering the horizontal accelerations in a way that mimics the performance of the stabilising platform, and then adding the contributions in a square sum. However, the square sum should include all modelled acceleration effects from all directions: Normal gravity, Coriolis effects and inertial accelerations.

2.3.4 Coriolis effects

Any object moving within a rotating reference frame is subject to a fictitious force called the Coriolis force. We recognise this as the final term in Eq. 2.11 (Torge and Müller, 2012). Coriolis force in the context of a local-level reference frame can be composed with e (East), n (North) u (Up) directionality (i.e. rotated to ENU). The magnitude of the Coriolis force depends on latitude and velocity. Note that the up direction is the same as the final two terms in the scalar observing equation 2.12, this is commonly referred to as the Eötvös effect:

$$F_{Coriolis} = \begin{bmatrix} F_e \\ F_n \\ F_u \end{bmatrix} = \begin{bmatrix} 2\omega(v_n \sin\varphi - v_u \cos\varphi) \\ -2\omega v_e \sin\varphi \\ 2\omega v_e \cos\varphi + \frac{v_e^2 + v_n^2}{R} \end{bmatrix} \qquad (2.13)$$

2.4 Filtering

2.4.1 The RC filter

The BGM-3 and some other sea gravimeters include an RC-circuit (resistor-capacitor circuit) within the readout electronics to filter out high-frequency signals. It works by limiting the amount of current that can pass through the circuit via a resistor in series and attenuates the resulting voltage by a capacitor in parallel following the resistor. It is an extremely common type of circuit used in electrical engineering, due to its simple construction and ability to condition signals.

RC-circuits have a time constant, τ, equal to the resistance multiplied by the capacitance of the circuit components. In short $\tau = RC$. τ represents how long it takes for $1 - \frac{1}{e}$ or 63.2% of the input voltage to propagate through the circuit. This is best visualised by a step response, where at first, the input and output voltage is zero, then the input is changed to 1 volt, and the output signal is shown to rise to 63.2% in τ seconds. Figure 2.3 shows the ideal pulse response of the RC filter implemented in the BMG-3. The intersect are clearly marked to facilitate a good intuitive understanding of how the filter responds to changes in a signal.

In modelling the perceived inertial accelerations of the gravimeter from GNSS measurements, the simulated signal must be subjected to the same RC-filter as that is present in the gravimeter. Failing to do so would result in extremely high amplitude signals in the accelerations, that appear to be offset from the gravitational observations by some negative phase shift. Since RC-circuits are analog in their nature, it becomes necessary to implement a discrete time approximation to the filter. Haugen (2008) has derived such an approximation which yields the following equation:

$$y(t_k) = (1 - a)y(t_k - 1) + au(t_k) \tag{2.14}$$

Where:

$$a = \frac{h}{T_f + h}$$

Haugen's equation (2.14) was implemented in a python function to simulate this RC-filter. In his paper, Haugen describes this type of filter as a low-pass filter, which is the *de facto* category of which these RC-filters are known to belong to.

2.4.2 Kalman-filter

A Kalman-filter is a general category of optimal filters that follow a particular algorithm designed to model a system's real-world behaviour (Kalman, 1960). Kalman-filters will be mentioned several times in this thesis but are not used.
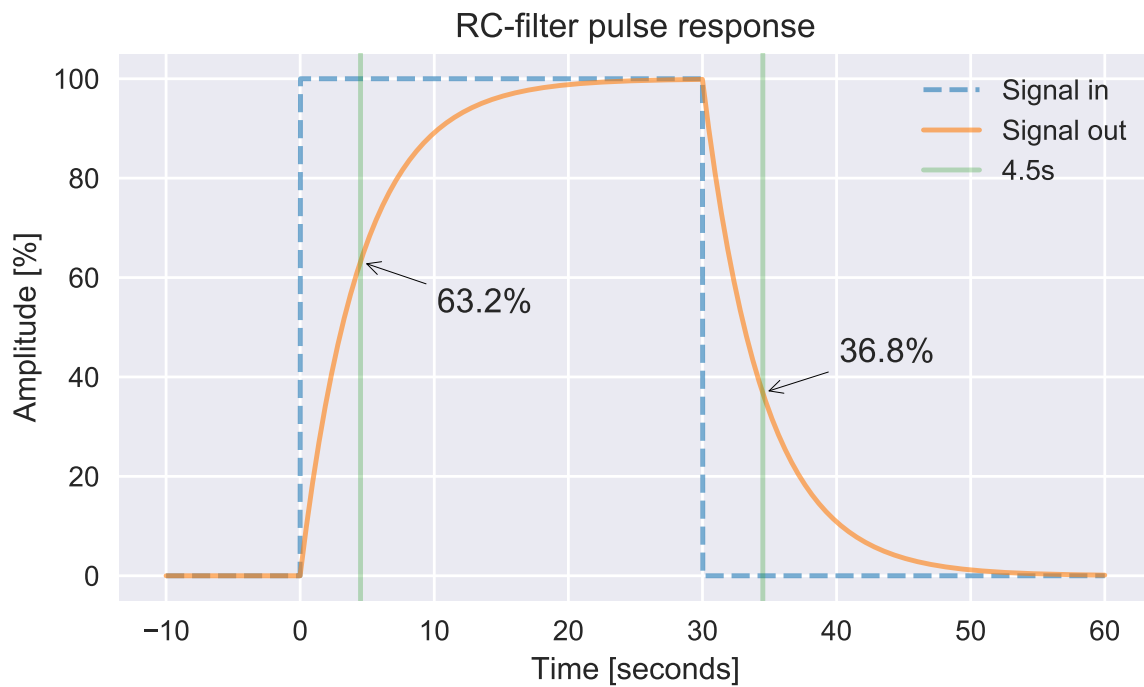
Figure 2.3: This figure shows the pulse response of an RC-filter with $\tau = 4.5s$ and a pulse width of 30 seconds. Green vertical lines indicate 4.5 seconds after a change in the input signal. This graph was generated using the same exact filter that is used to condition the modelled signals in the result section. Therefore it also represents the analog RC-filter embedded in the BGM-3

Chapter 3

Operating platform and instrumentation

3.1 Platform description

The operating platform contained in this study is the research vessel MS Hydrograf, which is owned by The Norwegian Mapping Authority (Kartverket) and operated by its Hydrographic Office in Stavanger. The ship is approximately 44 meters long, 10 meters wide, and weighs more than 640 metric tonnes. It can lift aboard small motorboats and often do so to transport the motorboats MB Lomvi and MB Havelle to support its mapping missions.

All sensors are positioned and referenced within the ships coordinate system 3.1, defined by a revised rapport from Parker Maritime AS following a dimensional survey in February 2008.

3.2 Instruments

The ship is inhabited by a Bell Aerospace BGM-3 sea gravimeter, whose measurements are the primary focus of this thesis. The BGM-3 is connected to a data logger computer which also receives navigational input from the ship. The Seapath navigation system from Kongsberg delivers a real-time GNSS+IMU solution to provide position and time

Table 3.1: Component coordinates

Component coordinates (all units in meters)			
Instrument	X - coordinate	Y - coordinate	Z - coordinate
Gravimeter	-2.185	-1.694	0.823
GNSS receiver A	-8.662	3.106	-13.802
GNSS receiver B	-5.766	3.217	-13.765
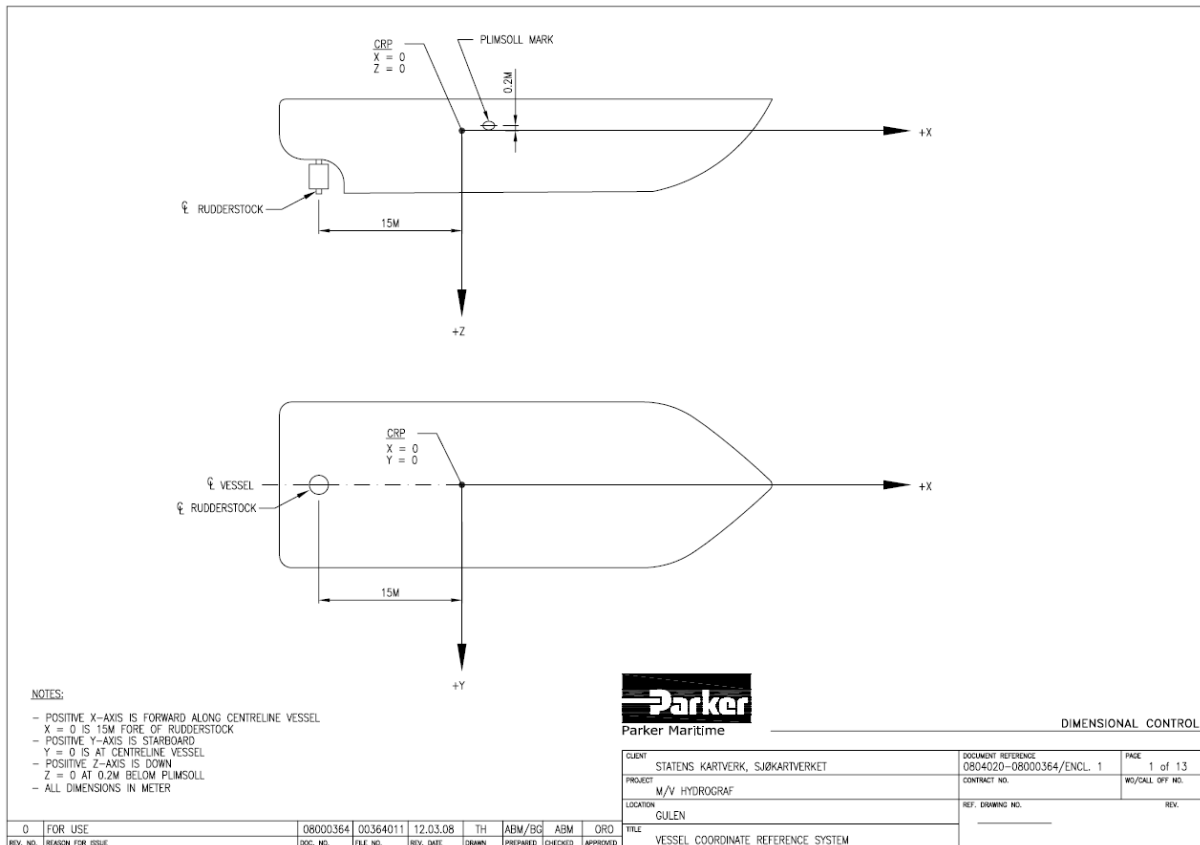
Figure 3.1: Definition of the coordinate system as measured by Parker Maritime AS

information to the gravimeters computer. This real-time solution is delivered to the gravimeter datalogger computer through NMEA sentences, that are logged together with the computer's internal time at a frequency of about 1 Hz. The computer's internal time is also used to reference the gravimetric readings, which also occurs at a rate of about 1 Hz. However, these rates differ slightly which causes the time difference to vary up to 0.5 seconds between gravitational and positional measurements. Incidentally, these timing irregularities accumulate to 3 seconds of "missing" data every 24 hours.

3.2.1 Bell Aerospace BGM-3 sea gravimeter

Even though the BGM-3 was installed in MS Hydrograf in 2015, the gravimeter is quite old. According to Bell and Watts (1986) this type of gravimeter was first available for academic use in 1984. The BGM-3 is a relative type gravimeter, optimised for use at sea. A more in-depth description of relative gravimeters is provided in section 2.3.1. The age of the instrument might affect its performance such as indicated by Peters and Brozena (1995). In this article, they describe the time coefficient, τ, of the internal RC-filter of their instrument to have changed from $\tau = 20s$ to $\tau = 19.5s$ due to ageing components.

The BGM-3 contains the same filtering component embedded in the readout electronics as
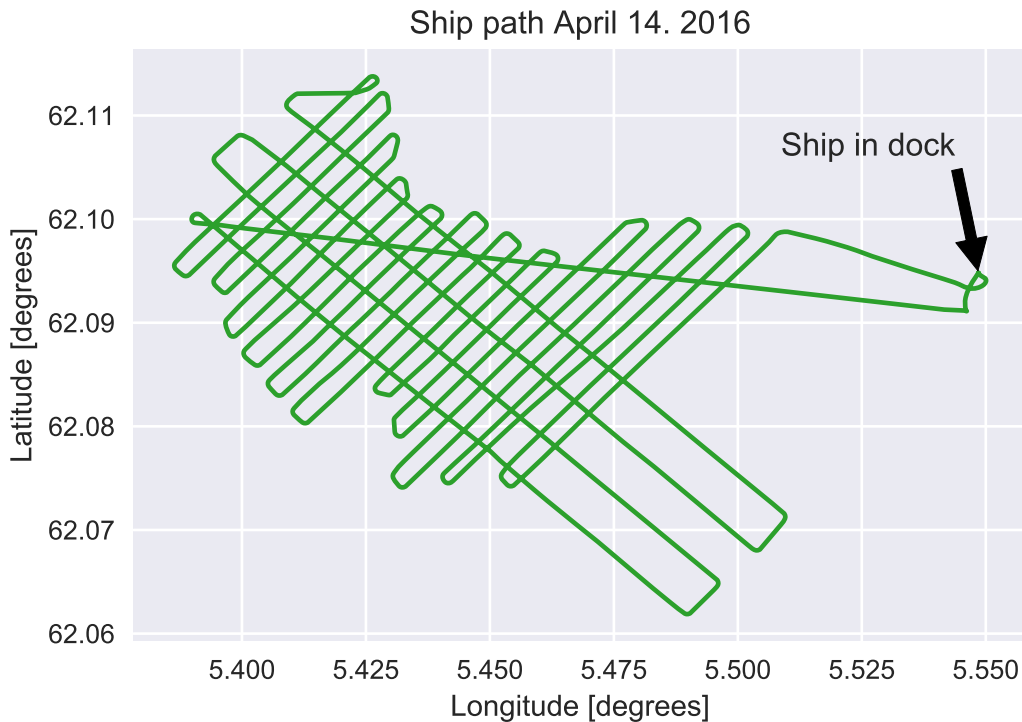
Figure 3.2: MS Hydrograf path during the observing period on April 14. The ship ends its survey by a long straight track across the entire observation area

the one described by in the article by Peters, but with a $\tau = 4.5s$ instead. The operational and maintenance manual of the gravimeter, as published by Bell (1979) states, on page four, that the readout electronics contain a "single RC lag" with a time constant, τ equal to "about 4.5 seconds." This wording can be misleading since the word "lag" can be read to mean delay. However, the purpose of this component is to prevent high-frequency signals from reaching the electronics, such that pulse rate converter is not saturated, as explained in the manuals section on filtering. The existence of this RC-filter in the BGM-3 is very significant for the development of method 2 and 3, and will be discussed further in section 2.4.1.

Unlike the more famous Lacoste-Romberg gravimeters, the BGM-3 does not sense gravity by a dampened spring system. It suspends an electromagnet in a permanent magnetic field by a "high gain second order servo loop" (Harlan, 1968). The output of the gravimeter is directly related to the voltage at which the electromagnet is subjugated. The sensor subsystem is contained on a gyro-stabilised platform, which again is contained within a double oven for constant temperature control at all times. The double oven configuration is designed to maintain a constant temperature both for the accelerometer but also for some of the signal conditioning electronics such as the RC-filter.

Additionally, Bell has provided a separate manual that describes the workings of the gyro-stabilized platform on which the gravimeter rests.

The two horizontal accelerometers on the platform have the capability to sense
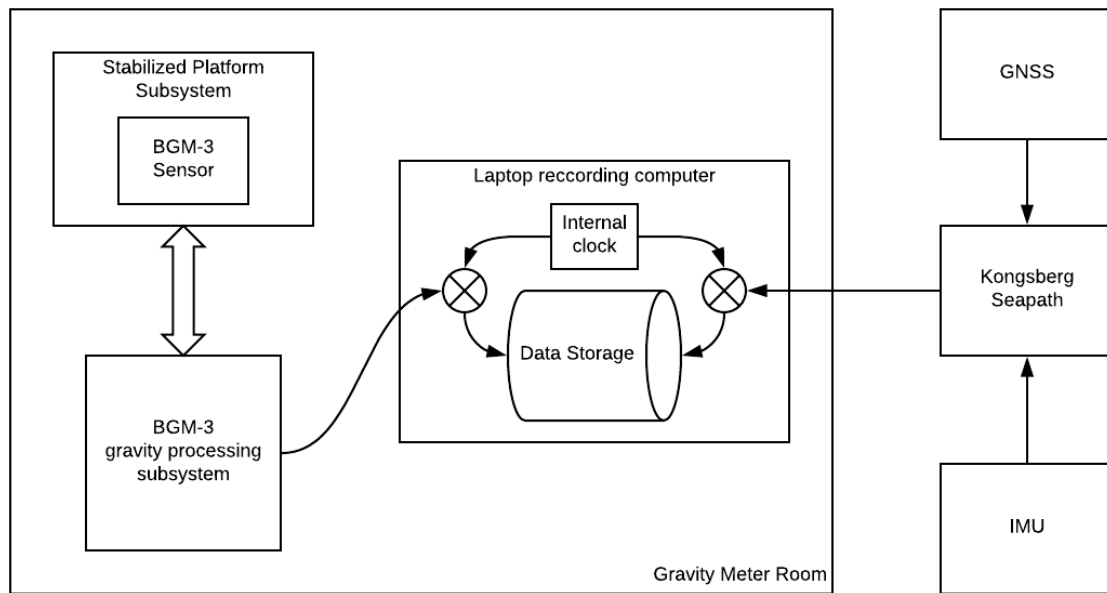
Figure 3.3: Relation between data sources and the logging computer on board the MS Hydrograf

> gravity, align the vertical sensor sensitive axis along the gravity vector, and sense horizontal accelerations in order to minimize their effects on the gravity reading. (Bell, 1987)

The gyro-stabilised platform attempts to maintain vertically of the gravity sensor, but what this vertically refers to is ambiguous in the manual. It claims to maintain vertically but hints that it will follow the plumb gravity vector. This could virtually eliminate small movements in the X-Y from ocean surface waves impacting and influencing the course of the ship. Conversely, if the ship makes an extended turn, the gimbal would after some time, not be able to distinguish the gravity vector from the centrifugal force vector.

3.2.2   Kongsberg Seapath

The NMEA sentences provided to the gravimeters datalogger are the result of an output from the ships onboard positioning solution. The Seapath integrates GNSS and IMU measurements to provide a real-time 3D solution including position and orientation. The NMEA standard published by the National Maritime Electronics Association and used to deliver data to the logging computer does not include a way to transfer orientation data. This means that only position is delivered. Position, not of the antenna, but of the origin of the ships coordinate system as discussed in section 3.1.

The Seapath system is also responsible on its own for logging GNSS and IMU information. This information can later be used for more accurate post-processing. E.g. as with TerraPOS.

15
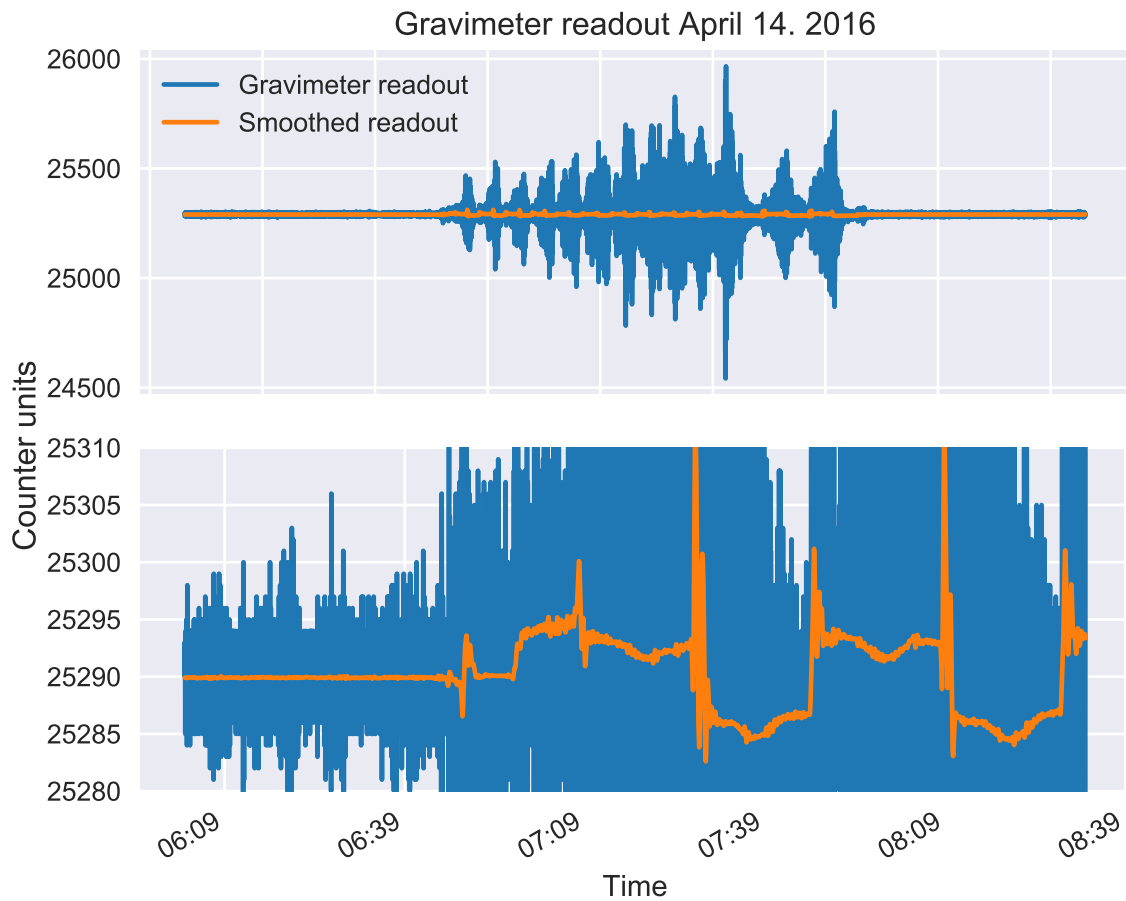
Figure 3.4: A visualization of data output from the BGM-3 gravimeter on March 14th 2016. The top view represent 24 hours of observations while the bottom shows the beginning of the surveying mission

3.2.3   TerraPOS

TerraPOS is a software developed by Narve Kjørsvik for TerraTec AS for post-processing of various GNSS and INS applications. Primarily the software works by integrating raw data from GNSS and INS (or IMUs) with precise satellite ephemerids and platform information in a Kalman filter process. This process, the Kalman filter, can best be described as an optimal filter that finds the most realistic estimates of the state of a system given measurements and system properties. A common example is to imagine a ship moving along a straight line, but a GNSS measurement shows a 'jump' 10 meters to starboard and then back on track in the course of three seconds. Depending on the size of the ship, let's say a container vessel, this deviation would be extremely unrealistic. The Kalman filter understands that its difficult for so much mass to move off track so fast and back again, and therefore delivers an estimate that practically disregards the false or noisy measurement.

In the context of this thesis, limited information is known about the parameters given to TerraPOS to calculate the 3D solution. Post processing was done by Lars Koren Nesheim at The Norwegian Hydrographic Service, a subdivision of the Mapping Authority in Stavanger, Norway. The tracks are calculated for the position of the gravimeter by the lever arm described in table 3.1, and provides not only position, but velocity, acceleration and orientation. The availability of this data is the foundation for the method using TerraPos data. A copy of the datafile header for the TerraPos exports can be found in Appendix A

3.3   Development

The development has largely been centred around Python 3.6 with Pandas 0.22.0 (McKinney, 2010), Numpy 1.6.1 and SciPy 0.19.1 (Jones et al., 01). In practice, Jupyter Notebook (Pérez and Granger, 2007) was as the integrated development environment (IDE). These citations are included for compatibility reasons. The code was developed to be function-orientated rather than object-orientated to create more easily understandable code that would be compatible with existing workflows.

Chapter 4

Method

This chapter will provide a detailed description of the processes of creating and evaluating Δg and δg observation from raw gravimetric data and navigation information from both the Seapath onboard navigation system and the post-processing software TerraPos. This chapter will cover the basic operations performed to obtain the results; it will not cover the specific functions in the processing script. That can be deduced from the example code in the appendix.

In traditional sea-gravimetry, the gravimeter's orthometric height above the water is considered zero. In effect, this means we assume the gravimeter is measuring on the equipotential surface of the geoid itself. The height of the instrument is assumed to be zero ($H = 0$). The advantage of this is that the number of possible uncertainties is kept to a minimum. Conversely, if we consider the recording situation to take place with respect to the ellipsoid, the gravimeter would be referred to a height above the water, and these observations would be in the same reference system as land and air-borne gravimetry.

4.1   Overview

The investigation herein revolves around corrections that can be made to the scalar gravity readout to improve results. This is done by estimating what the what the gravimeter senses as its platform moves around on the ocean. This estimation is complicated by the gravimeter's position in the ship, the gyro-stabilised platform on which it rests, its sensitivity, drift, and internal signal conditioning. The proposed vector equation to account for these effects (eq. 2.11) is herein simplified to:

$$g = \gamma + F_{Coriolis} + a_{Platform} \tag{4.1}$$

expanded in matrix notation:

$$g = \begin{bmatrix} 0 \\ 0 \\ \gamma \end{bmatrix} + \begin{bmatrix} 2\omega(n\sin\varphi - u\cos\varphi) \\ -2\omega e \sin\varphi \\ 2\omega e \cos\varphi + \frac{e^2+n^2}{R} \end{bmatrix} + \begin{bmatrix} \ddot{x} \\ \ddot{y} \\ \ddot{z} \end{bmatrix} \qquad (4.2)$$

To reiterate, all of these direct effects reflect forces acting on the gravimeter unit. However, the sensor unit is on a stabilised platform and is subject to both mechanical and electrical filtering. Thus, the modelled signal must be filtered in the same way as the real world accelerations are. We can only approximate, but the idea is to leave as little else than the gravity signal as possible. Ultimately the model is subtracted from the observations such that:

$$\delta g = g_{obs} - model \qquad (4.3)$$

Where the *model* is:

$$model = \gamma_O + F_{Coriolis} + a_{Platform} \qquad (4.4)$$

To be clear, *observations* refer to the information coming out from the gravimeter (see figure 3.3). The **model** is essentially what we need to subtract from g_{obs} to obtain anomalous gravity.

4.2   Observation

Readouts from the gravimeter are provided in *counter units*, an arbitrary unit specified to be linearly proportional to acceleration with a scale factor:

$$CU_{scale} = 4.911302 \frac{mGal}{CU}$$

Counter units are always integer, meaning that the minimum step the BGM-3 can deliver is 4.9 mGal! (This detail was also pointed out in Bell (1979)) In addition to scaling, a gravimetric readout must be fixed to a reference point. In this case, the reference point was chosen to be a quay in Bergen and details are provided by Omang (2017). This scaling and fixing procedure can be described by:

$$g_{ref} = g_0 + (CU_{read} - CU_{base}) \times CU_{scale} \qquad (4.5)$$

Where g_{ref} becomes the referenced measurement in $mGal$, CU_{read} reflect each measurement readout from the gravimeter in counter units and CU_{base} refers to the counter value readout at the reference time. g_0 represents the gravity at the tie point at the same time as CU_{base}, but differs depending on which reference is used. In traditional sea gravimetry and indeed in the control method, g_0 is the gravity value on the geoid, or rather on the surface of the ocean, as the two are considered coincident. In this case, a free air reduction

is performed on the quay base point to calculate g_0 at the level of the water (orthometric height, H, equals quay height).

In the case of using the ellipsoid as a reference plane, g_0 is not considered to live on the geoid, but rather at the same ellipsoidal height as the relative gravimeter. The base reading is in that case reduced by the free air gradient of the height difference between the relative gravimeter and the point of the base reading. The ellipsoidal height of the relative gravimeter (h_{BGM3}) can be obtained from the lever arm corrected GNSS positioning provided by the Seapath system. Note that ellipsoidal height of the base reading (h_{base}) must also be obtained. For these referenced measurements to be valid over an extended period, they must be drift-corrected.

4.2.1 Drift reduction

The BGM-3 Bell relative gravimeter is, as discussed in the introductory chapter, subject to drift. This effectively means that a drift parameter can be calculated and added to the referenced observations, g_{ref}. In this case, drift has been calculated by linear propagation from the gravity tie point such that:

$$P_{drift} = (t - t_0) * P_{rate} \qquad (4.6)$$

$P_{rate} = 0.066 \frac{mGal}{day}$, as provided by Omang (2017). Where t and t_0 is measurement time and calibration time respectively. Torge and Müller (2012) and Bell and Watts (1986) suggest that a low order polynomial be used to estimate drift. The implemented python function to estimate linear drift can be found in Appendix B. To construct the referenced and drift corrected gravity observation, g_{obs}, one need simply add them together:

$$g_{obs} = g_{ref} + P_{drift} \qquad (4.7)$$

4.3 Creating the model

Different considerations apply in the case of traditional sea gravimetry than for methods referenced to the ellipsoidal. However, these differences pertain only to the estimation of the normal gravity ($gamma$), which in the case of the former, is estimated with no ellipsoidal height $h = 0$. While in the case where gravity is referenced to the ellipsoid, ellipsoidal height of the instrument is used directly.
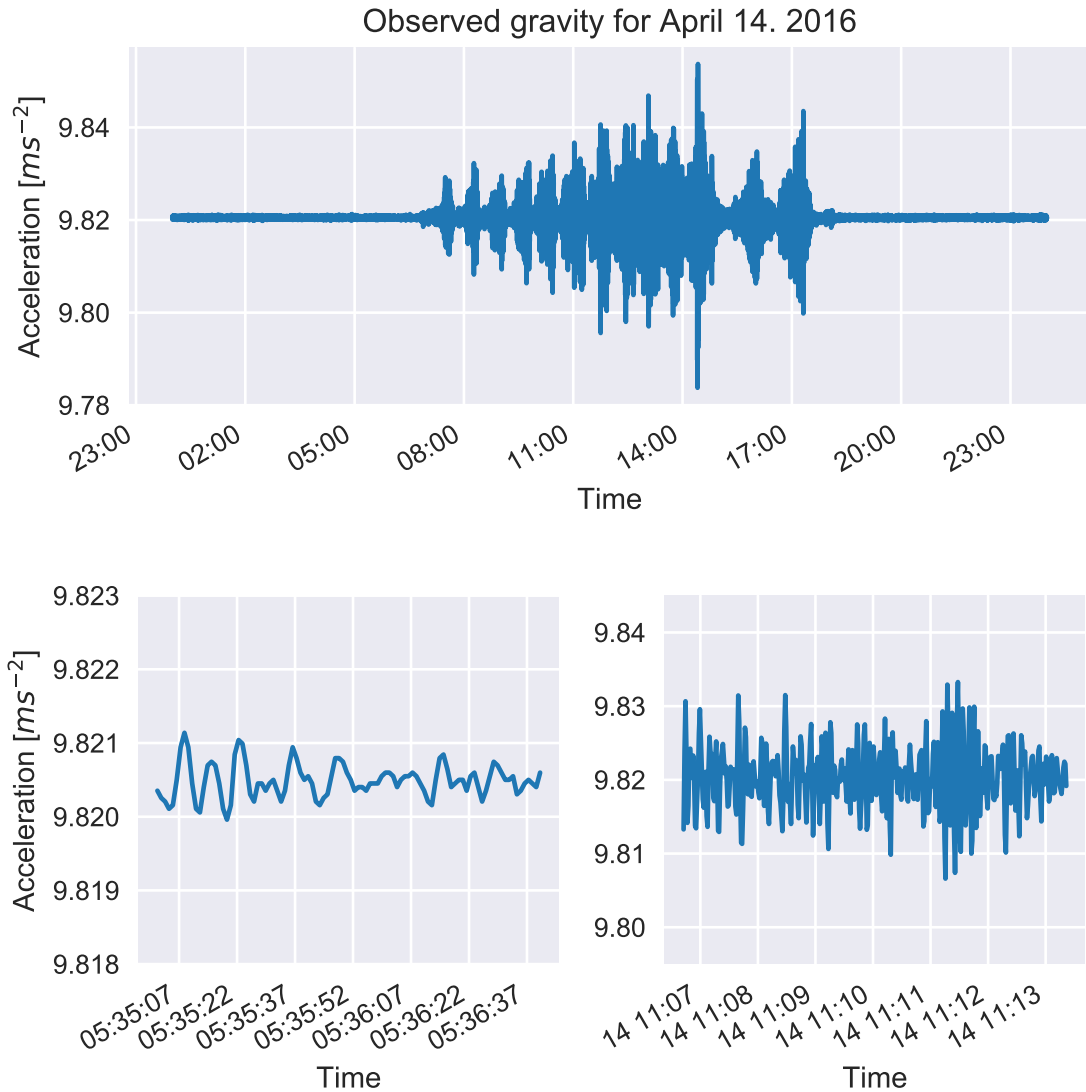
Figure 4.1: Gravity as recorded by the BGM-3 and drift adjusted for March 14. 2016. The top figure shows the variations in gravity over the entire day while the bottom two show common variations in records from a time where the ship is at a dock (left) and when the ship is on a campaign (right). Variations are close to hundreds when the ship is not moving and over a thousand mGal while it sails.

4.3.1 Normal Gravity

The first implementation of normal gravity uses the latitudinal position and ellipsoid height as recorded by the GNSS receiver to calculate the normal gravity on the GRS80 ellipsoid (Python function provided by Ove Omang). Ellipsoidal height, h, of the gravimeter is used for calculations not relating to the traditional processing method.

4.3.2 Coriolis effects

In the ENU local-level reference frame the Coriolis effects are calculated based on the first derivative of position (velocity) in three dimensions. The derivative calculation takes place in the ECEF reference frame and is rotated to the local level ENU coordinate system. Additionally, the upwards Coriolis component, or Eötvös component, is supplemented by the centrifugal effect ($\frac{e^2+n^2}{R}$) experienced while moving across the surface of a sphere. $F_{coriolis}$ is calculated by:

$$F_{coriolis} = \left[\begin{array}{c} F_{north} \\ F_{east} \\ F_{eot} \end{array} \right] = \left[\begin{array}{c} 2\omega(n\sin\varphi - u\cos\varphi) \\ -2\omega e\sin\varphi \\ 2\omega e\cos\varphi + \frac{e^2+n^2}{R} \end{array} \right] \tag{4.8}$$

4.3.3 Platform acceleration

Platform accelerations are calculated directly by the second derivative of position with respect to time. The calculation is performed in the ECEF reference frame, and the resulting acceleration vector is transformed to a local level ENU coordinate system. However, before this calculation is performed, a prefiltering of recorded position takes place: Wei and Schwarz (1995) shows using a Kalman-filter before differentiation. In place of this, the Seapath system (in all likelihood) contains a Kalman filter, but it supplies coordinate heights truncated to centimetres. This means the resulting signal is step-like. To moderate artefacts in the second derivative, a Gaussian prefilter convolution smooths the positions provided by Seapath.

4.4 Signal conditioning

For the model to correctly estimate the gravimeter's readout, other than the actual signal containing information about δg, each component in equation 4.2 must be filtered appropriately. By analyzing each effect in turn and by deducing how each effect must act the test mass, it is possible to build a model that will estimate the readings of a moving gravimeter on the ellipsoid.

After the vector model has been collapsed to a scalar model, it must undergo signal filtering that mimics the internal electronic filtering of the readout electronics, namely the
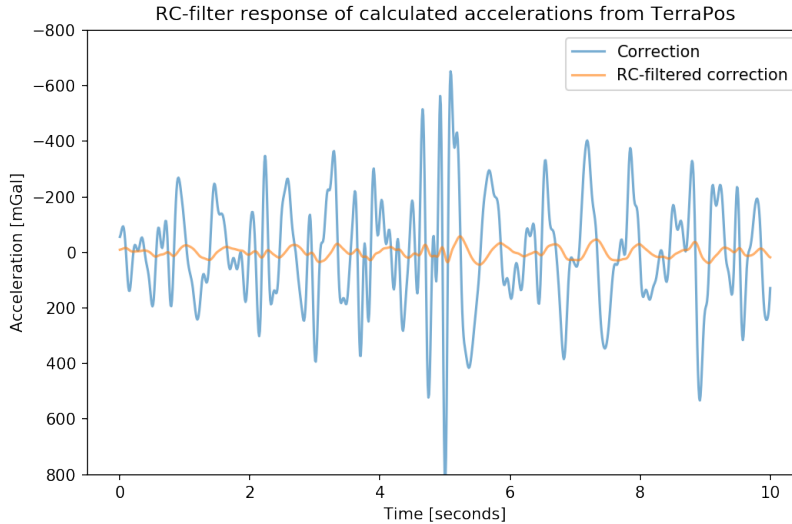
Figure 4.2: Application of the RC-filter on accelerations produced by TerraPos. The filtered signal can seam to lag behind the input by a quarter period or 90 degrees

RC-filter (section 2.4.1). Then, a smoothing filter must be applied to both the observations and the model to remove any remaining phase offsets and to define the resolution of the resulting δg output.

4.4.1 Component filtering

γ can be shown to vary on the order of 1 mGal as a result of height variations and not more than 5 mGal during the case study day. Small variations do occur, but they are not significant to warrant any filtering. Therefore the γ component is not filtered.

Conversely, Coriolis effects routinely have variations that span 50 mGal. The effects of North and East components of the Coriolis effects warrants further discussion (see Results section) but the vertical, or the Eötvös effect, affect the gravity sensor directly, i.e. there is no reduction in its effect on the gravimeter unless the gravimeter is tilted. This suggests that Eötvös effects do not need to be filtered.

Acceleration is another problem entirely, due to the nature of the gyro stabilised platform which is supposed to suppress effects of horizontal accelerations. It does this on effects that are short enough in duration (high frequency), but fails to sustain verticality in long-duration turns where the acceleration due to centrifugal effects slowly displaces the perceived downward pointing gravity vector. This causes the observed signal to rise to a peak in between straight tracks. I.e. some of the additional acceleration from the centrifugal effects of the turn is added to the measured gravity scalar. However, results show that horizontal accelerations can be used to reduce peaks in the observed data during a turn but not eliminate them completely. For now, testing suggests applying a powerful low-pass filter to the horizontal (East and North) accelerations. In other words, their impact on the gravimeter's readout is not fully understood: We can see high amplitude

signals in the horizontal accelerations making it through to the sensor, but we know high-frequency signals are compensated for by the platform. More on this in the discussion chapter.

Vertical positions are often more inaccurate then horizontal positioning. This added uncertainty propagates to the second derivative also. Additionally, the positioning data from Seapath and TerraPos merged GNSS data with data from an IMU. We know from Eq. 2.12 that vertical accelerations affect the gravimeter directly, but from initial tests, it was discovered that in this case, direct addition of the vertical accelerations caused some periodic oscillations in the model that are not present in the observed gravity (g_{obs}). Therefore a high-pass filter has been applied, designed to limit a_{up} to above 0.08 Hz or 12.5 seconds, the frequency expected to contain signal from ocean surface waves.

4.4.2   Collapsing the vector equation

To create a scalar model of what the gravimeter senses, i.e. before analog signal filtering (RC-filter). Vector contributions can be added together before all directions are square summed. In the results section, one model is constructed for all 3D effects with Seapath data, one with the TerraPos data, and one model with only the vertical components, only from the Seapath data are constructed. The control model is constructed only from the normal gravity at the ellipsoid γ_Q, and the Eötvös effects. The models, with the appropriate pre-filtering, are then passed through the final filtering step (RC-filter) to estimate the gravimeter's output more appropriately.

4.4.3   Filtering the model

The scalar model for what the gravimeter senses has now been created, and what remains is to condition this model in the same way that the gravimeter conditions its inputs. This is done by emulating the built-in RC-circuit in the gravimeter's readout electronics. A discrete function has been construed based on Neumeyer et al. (2009). It is vital for the operation of this function that none of the input values is "NaN" (Not a Number). If the RC-filter is not applied to the model, amplitudes from acceleration would far exceed that of the observed signal and would seem to lead the signal by a phase offset of 90 degrees as shown in figure 4.2.

4.4.4   Subtraction of the model

To obtain the useful gravimetric values Δg and δg, the conditioned modelled signal must be subtracted from the gravimetric observations. This can be accomplished in two ways: First, by directly subtracting, which will leave a noisy-looking signal that subsequently must be filtered.[1] Second, both signal and model can be filtered separately, defining the

---

[1]The resulting track has variations that far exceed the expectation of the gravitational field. Results from when the ship is stationary have a standard deviation above 60 mGal

resolution of the result, before they are subtracted. This should help to prevent any remaining phase offset from cluttering the result, but tests have shown that subtracting the model from the signal before filtering yields the best results so long as they are correctly aligned.

4.5 Spectral analysis

To analyse comparatively model and signal, we generate a power spectrum by the use of SciPy's Lomb-Scargle implementation. This method is more robust than a Fourier transform because it can handle missing data-points and does not require equidistantly spaced observations (Scargle, 1982). In the result section, the spectral power axis has been converted from $mGal^2/Hz$ to dB using $10000mGal^2/Hz$ as a reference in order to provide a more intuitive plot for understanding signal strength at various frequencies.

Chapter 5

Results

This section discloses various results attained form the different considerations to reach the objective. To reiterate, the objective of this thesis is to develop a method of improving the raw data from the BGM-3 sea gravimeter onboard MS Hydrograf. In this respect, the objective has been achieved however, as the following sections will unveil, there may yet be additional room for improvement.

5.1 Control method

The significant difference between the control method and the investigated methods is the way they are referenced. The former is referenced to the geoid directly and uses a normal gravity at the ellipsoid, γ_q, while the latter uses normal gravity at the ellipsoidal height of the instrument, γ. Subtracting the two $\Delta\gamma = \gamma_q - \gamma$ yields an average offset of $\Delta\gamma = 13.9 \pm 0.4 mGal$, with variations that are due to change in height as the ship moves about. Functionally we can treat this as a 14 mGal offset when performing comparisons.

The results of the control method are shown in Figure 5.3. These results have undergone filtering by a convolution of a Gaussian bell curve, with $\sigma = 16$, and were then filtered by linear convolution with a length of 32 seconds, limiting the spatial resolution to just under 100 meters. A resolution of 0.1 km is what Bell and Watts (1986) claims to have achieved with the BGM-3. We can see from the figure that the gravity anomaly or disturbance decreases towards the centre of each pass across the surveying area, and spikes in the extreme when the ship is performing turns.

Figure 5.4 serves to illustrate how the control method tackles high frequencies. We can see strong contributions from high frequencies in the unfiltered data. These contributions are noise. Noise, which is made up in part by platform accelerations, which has not been accounted for in this method. However, we can observe that the two-step filtering process is suppressing the high frequencies. The drawback of this method is of course that the resolution remains coarse.
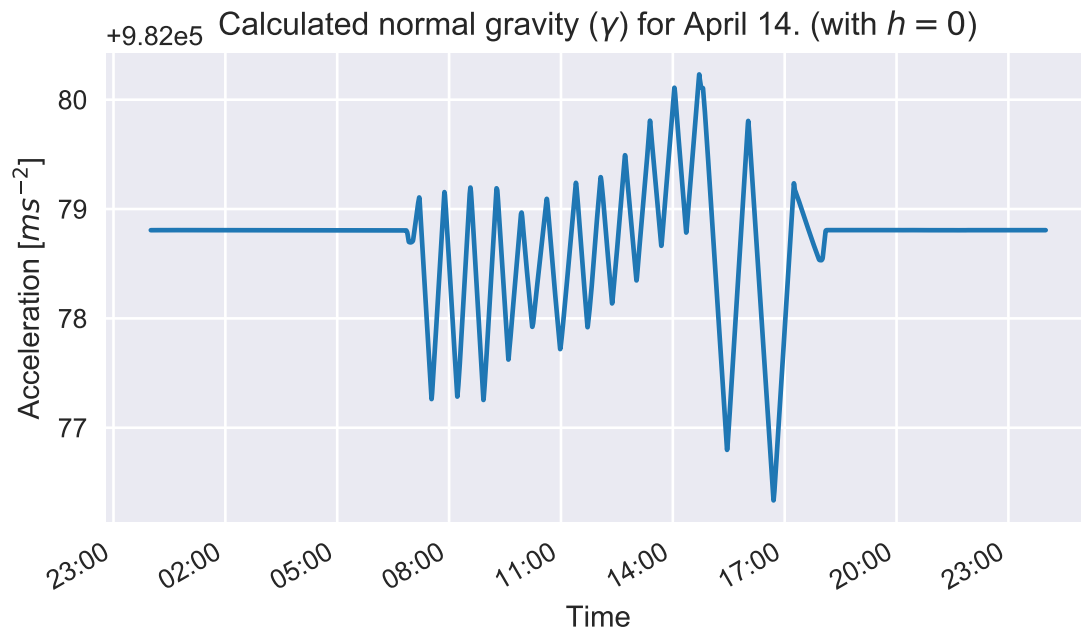
Figure 5.1: Normal gravity, γ, calculated for position along the track for March 14th 2016
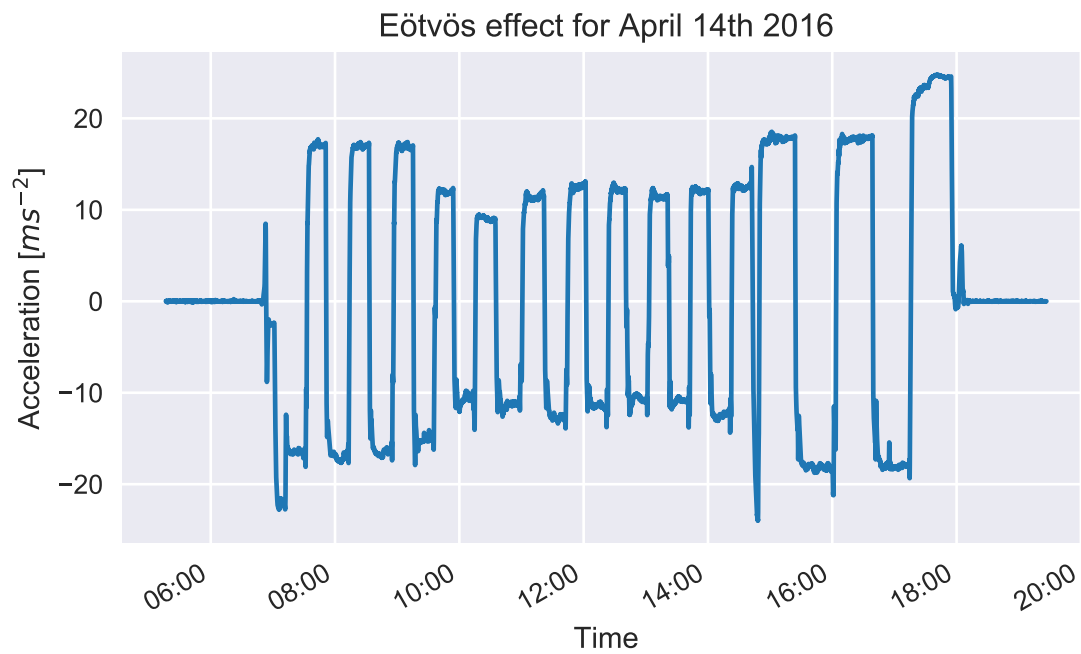
Figure 5.2: Calculated Eötvös effects from velocity derived from Seapath positions for operational hours on March 14. 2016.
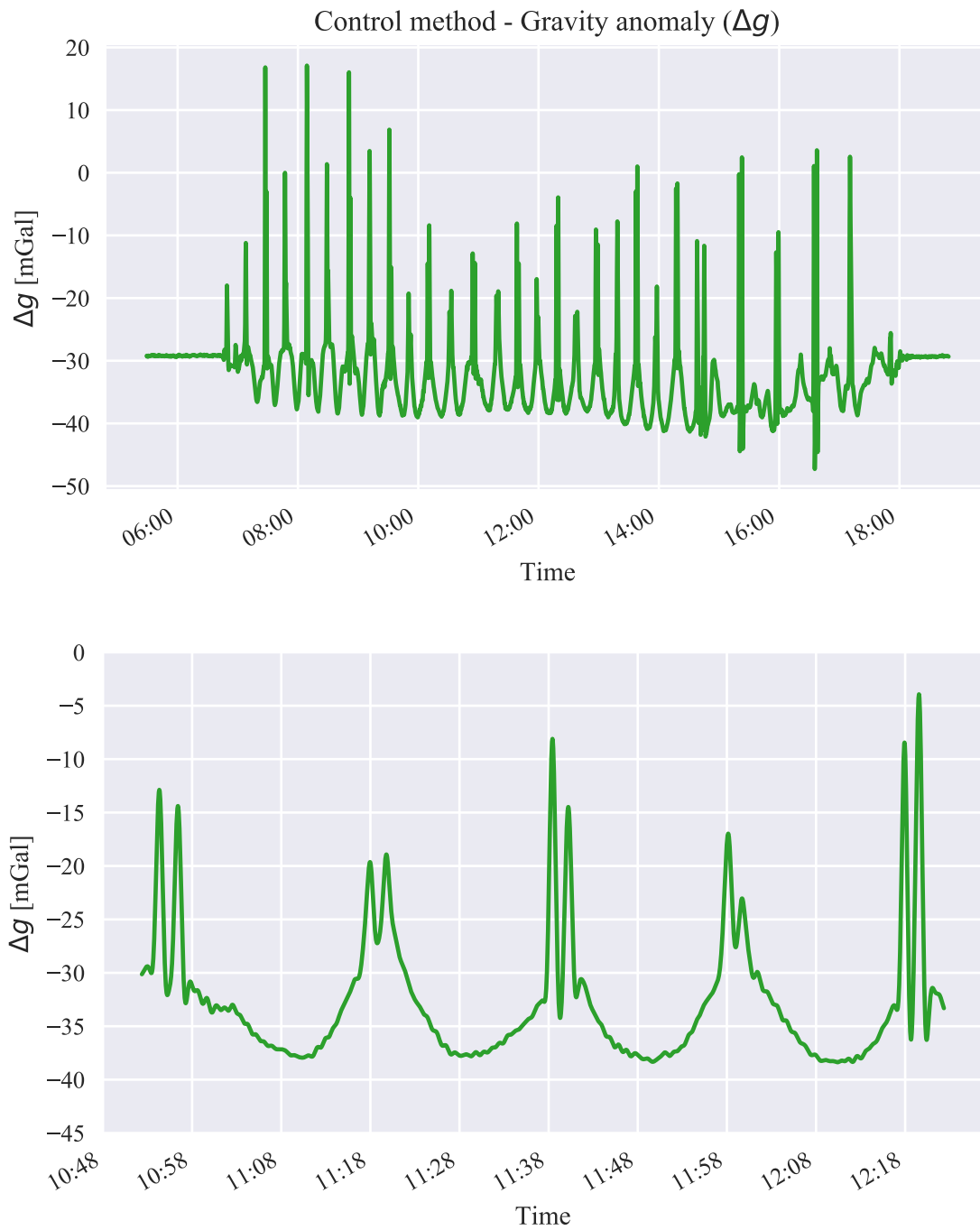
Figure 5.3: Resulting gravity anomaly for control processing method. The signal has been filtered extensively using both Gaussian and linear filters.
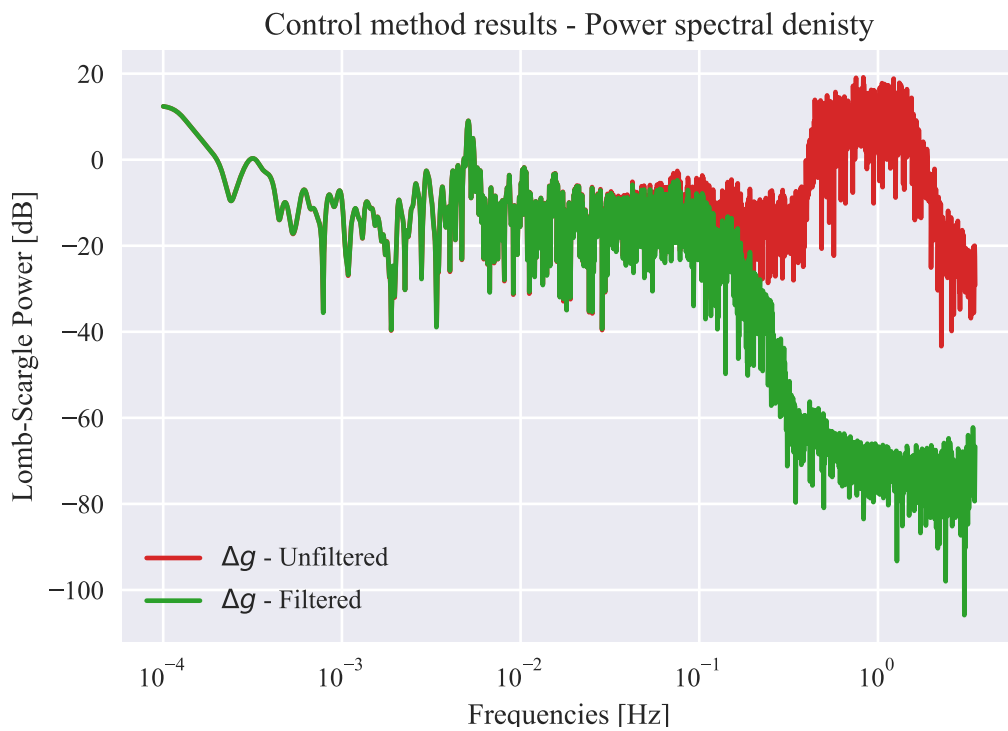
Figure 5.4: A periodogram of the control method, showing the Lomb-Scargle response across a range of frequencies. ΔgF is the response of the filtered data which is the product of the control method. The highest peack is located at about $5 \times 10^{-3} Hz$ which equals a period of 200 seconds.

5.2   Method using Seapath data

The Seapath data are presented here in two considerations: First, following the scalar observing equation (Eq. 2.12), which are expected to outperform the control method are presented in Figure 5.5. These have the same characteristics as the control method in that there are spikes in the data where the ship is turning. Second, following the vector considerations laid out in equations 2.11 and 4.2, the results of the new method with vector considerations using Seapath data are shown in Figure 5.6.

Notice the difference in the amplitude of the spikes from Figure 5.3. In Figure 5.5, the spikes seem to have decreased in amplitude, while in Figure 5.6 the artifacts are almost gone. Keep in mind the scale of the y-axis of these plots, as they vary to fit the data. We can see from all three plots so far that the middle of each track dips down about 15 mGal, presumably due to the increased depth in the middle. We can also observe that the scalar considerations (Figure 5.3 and 5.5) both have spikes that point upward, indicating more perceived gravitation than modelled gravitation. The vector considerations, on the other hand, have some spikes that point down, indicating that the model has estimated a higher gravity value than what the gravimeter has perceived. However, this seems to only be the case at the end of the observing session, or when the ship performs five cross-over runs.

5.3   Method using Terrapos data

The results from the TerraPos data are puzzling. Since it is a post-processing solution, we expected these results to be better than the Seapath solution. Remember, the accelerations and velocities are exported directly from the TerraPos software itself, and used in place of the derivatives of position. We would expect this to be more accurate since TerraPos uses a more comprehensive Kalman filter to determine these values. But what we see in Figure 5.8 contradicts that. It would seem that the corner spikes have been severely amplified in both directions, diverging up to 80 mGal off the track in both positive and negative directions. If the contributions from vertical accelerations were too large, we would expect all the spikes to be negative, but only some of them are. The positive spikes seem to have the same basic profile as in figure 5.3, but the amplitude is significantly higher.

The TerraPos data were exported from TerraPos with a higher temporal resolution of 10 Hz. The intention was to see if the increased resolution in time would help identify inertial accelerations from interactions with surface ocean waves. Of course, the resulting TerraPos model had to be resampled to 1Hz to be compared with the observed signal. The result of this can be seen in the spectral characteristics depicted in Figure 5.9 where it would seem that the unfiltered signal looks more detailed at higher frequencies when compared to the unfiltered signal of the other methods. Notice also that more of the signal peaks above 0 dB compared with the other signals.
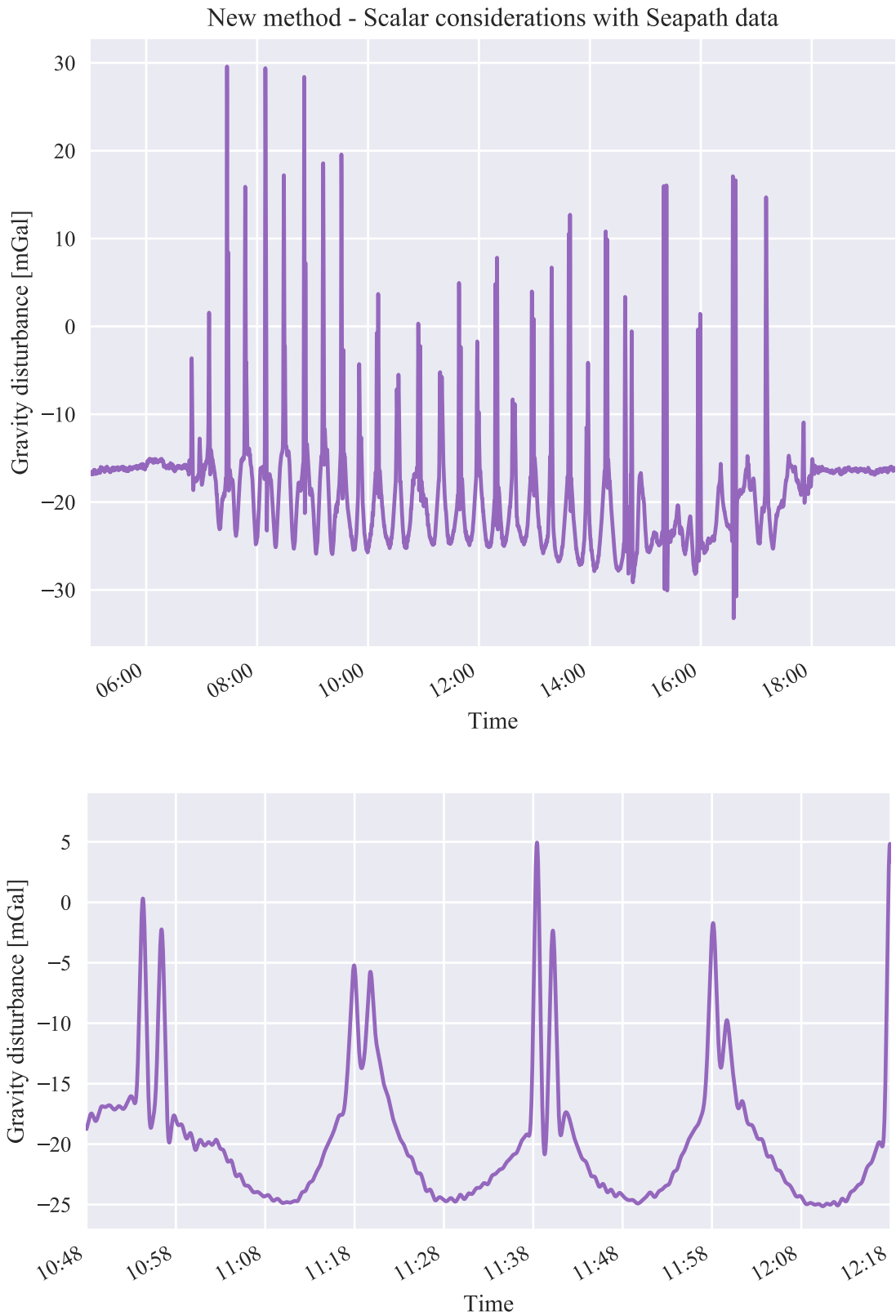
Figure 5.5: Gravity disturbance calculated using Seapath data and scalar considerations. Only components that are vertical with respect to a local level reference frame are used to produce these results.
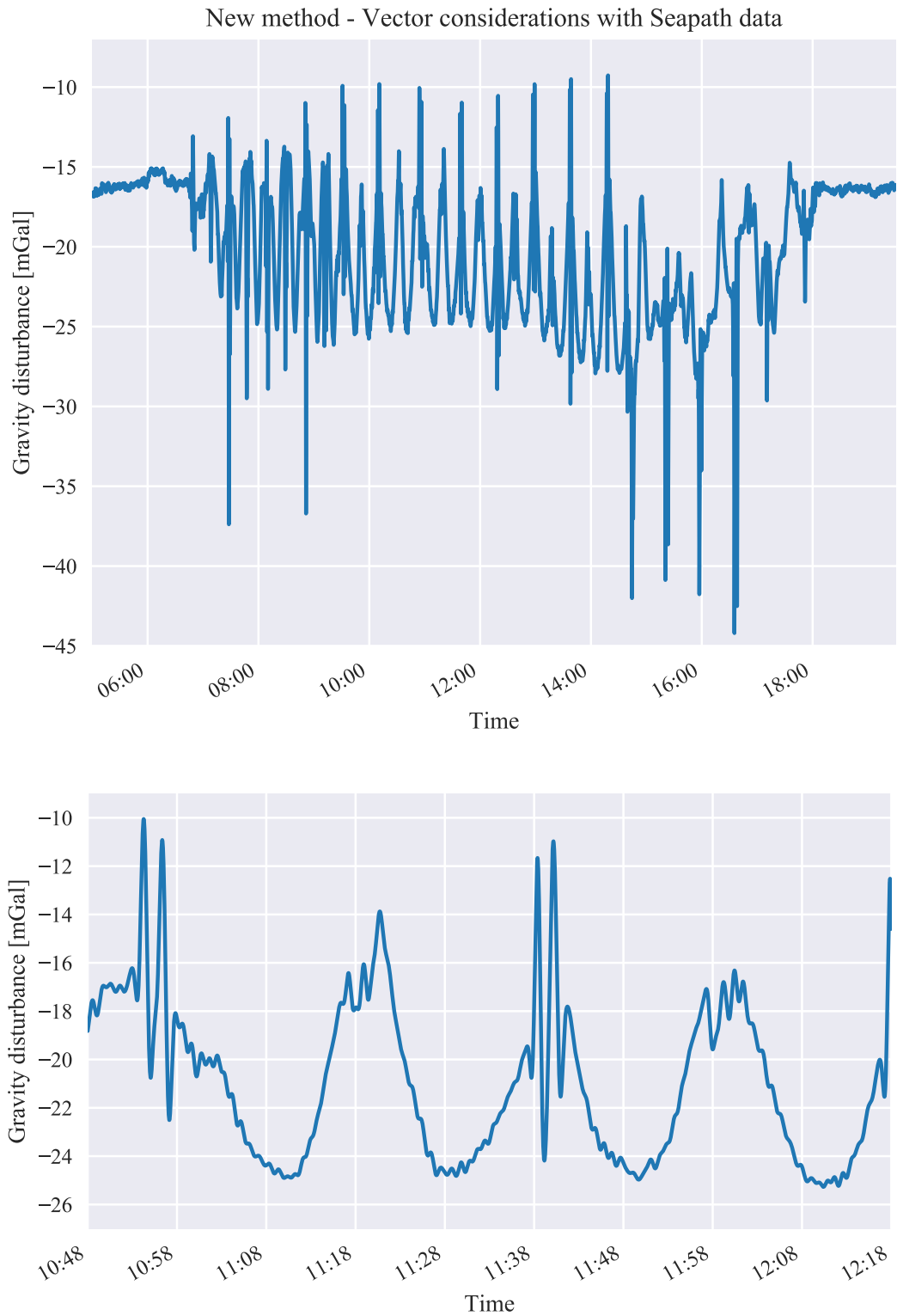
Figure 5.6: Gravity disturbance calculated using Seapath data and vector considerations. Components from all directions in the local-level reference frame have been used. Although differently filtered, this configurations seem to outperform the scalar consideration.
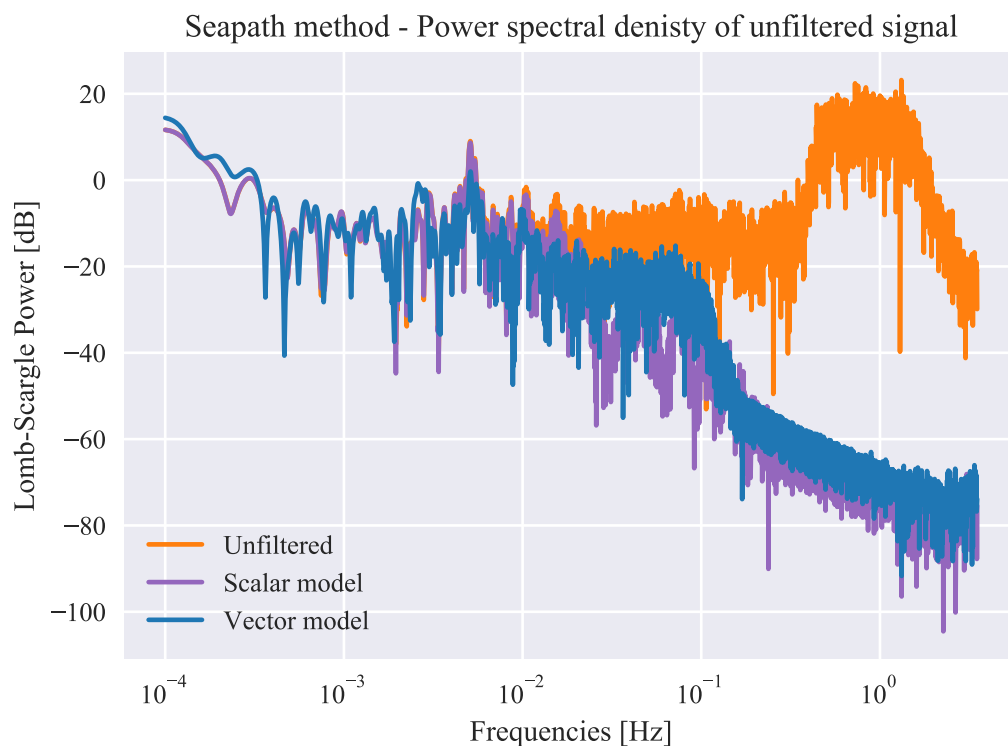
Figure 5.7: Periodogram showing the relative spectral contributions to the signal for the vector and scalar models. Note that the unfiltered PSD profile would be the same for both the scalar and the vector model
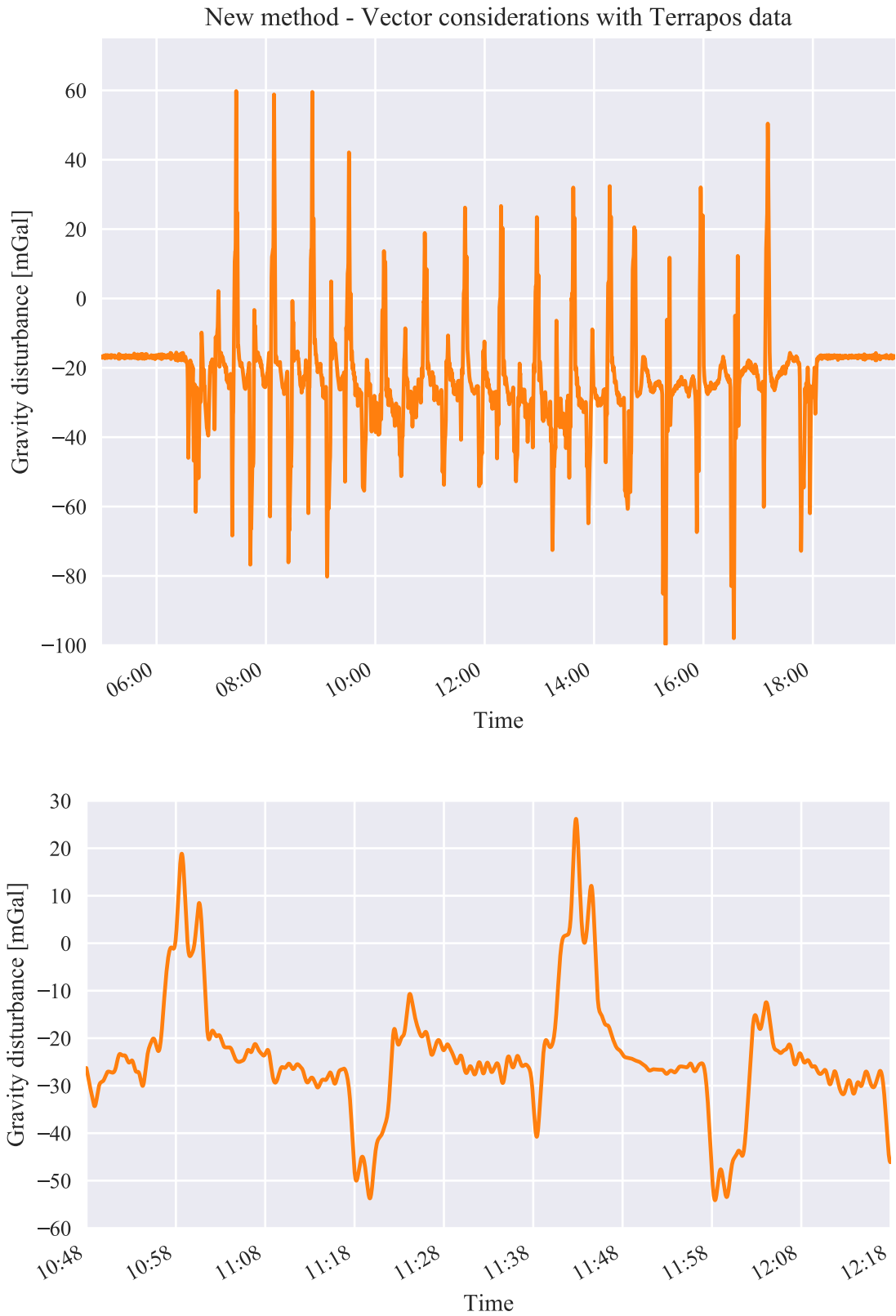
Figure 5.8: Gravity disturbance calculated using TerraPos data with vector considerations. The data seem to have a much higher variation than the control
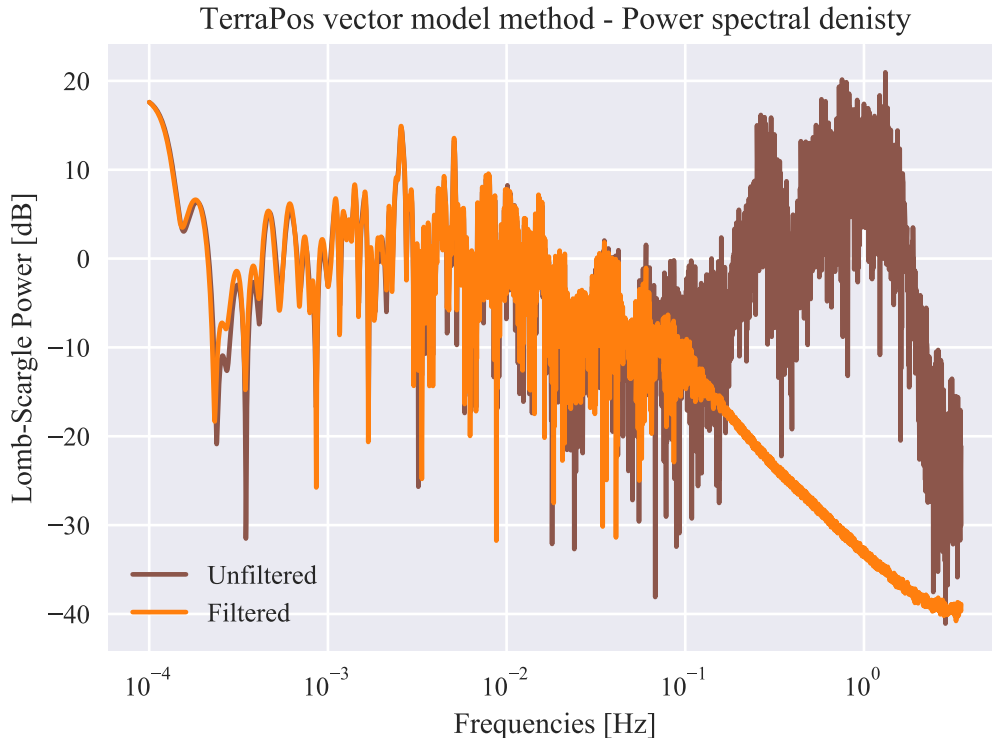
Figure 5.9: Power spectral density of the vector model used on the TerraPos data. Notice the strong contibutions above the zero dB mark

5.4 Relative comparison of models

Figure 5.10 compares the control method with the Seapath and TerraPos vector results. Imidiately, it becomes clear that the results produced by the TerraPos model have more variation than the two others. Again, since we expect TerraPos data to handle short accelerations better, this result is unexpected.

Moving on to the results from the Seapath data, we can see that they perfectly follow the profile of the control data along each track and that they have smaller variations when the ship is turning. This is a net positive result for the Seapath vector model, but it would seem that the variations along each track are slightly stronger than that of the control. An even closer inspection reveals that the Seapath results and the control sometimes diverge slightly on a line. This is believed to be due to the Coriolis effects in the horizontal direction, however, this effect is minute.

Taking a look at the models themselves, in figure 5.12, rather than the result we see something interesting. The TerraPos model does not seem to have an end of the line problem as we saw in figure 5.10. This holds true for the entire observing session and not just the outcrop which confirms that the flaw lies in the interpolation of the signal. Again, we see that the TerraPos model has more variation or more noise than the other models. This is in all likelihood related to accelerations, whether it is more noise in the accelerations themselves or improper handling is hard to tell. However, accelerations in
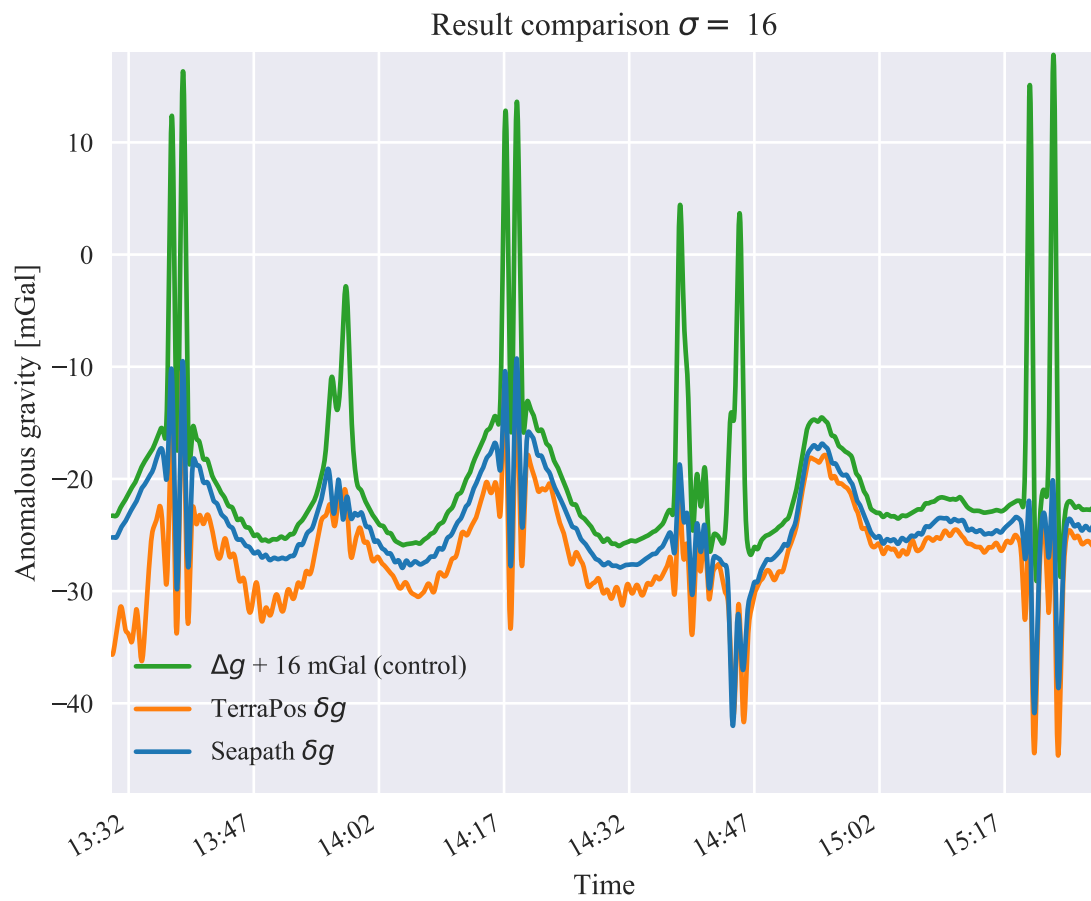
Figure 5.10: Comparison of results at $\sigma = 16$ or 90m resolution.
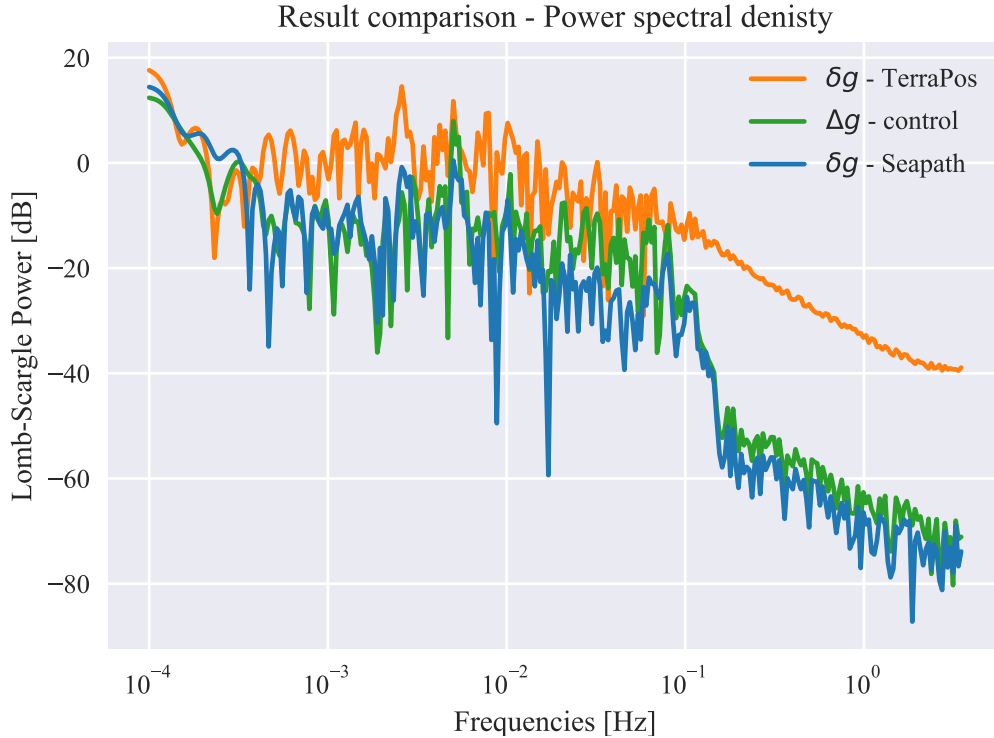
Figure 5.11: A comparison of power spectral density of the models

turns seem to be handled very similarly in both the TerraPos and the Seapath model.

Figure 5.12 also show the difference between the vector and scalar Seapath models. Notice how the scalar model overlaps the Seapath vector model during the track and how the vector model follows the contours of the observations during the turns. This is evidence that the vector considerations do not have a negative impact on the result along the track. In other words, the impact of vector considerations on a scalar graivmeter are not negative.

The track labeled "Observations" in figure 5.12 may warrant some explanation. It is the BGM-3 observations, g_{obs}, filtered with the same Gaussian filter as the compared models. It serves primarily to show how the gravimeter behaves in turn, such that the models can be compared. However, it also provides visual insight into the nature of gravity anomaly, which we have defined to be the difference between measured and modelled gravity.

Figure 5.13 show the the terrapos and seapath vector models against the actual observations made by the gravimeter. Both models have undergone filtering by the RC-filter in order to be compared but the TerraPos model has been filterd additionally. We can do this filtering because the TerraPos data are logged at 10Hz, and we have more resolution to work with in the time domain. Notice how the phase of both models seem to correpond perectly. This is somewhat of a trick with respect to the Seapath data; they have been offset by 0.5 seconds in relation to the observations. More importantly, notice that for both models, the amplitude sometimes fit perfectly. The Seapath model has a tendency to have too small amplitudes, and the TerraPos model has a tendency to exceed
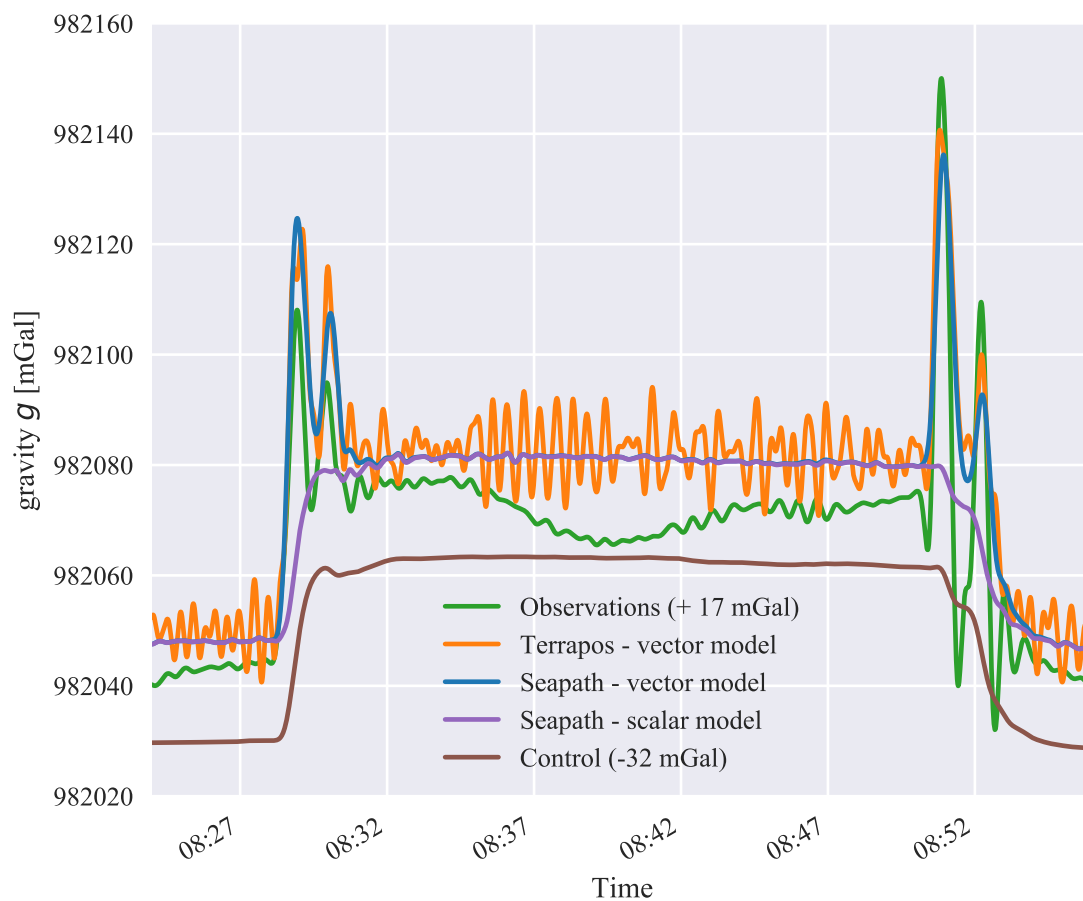
Figure 5.12: Comparison showing how vector considerations better estimate the peak signals from turns. All models and signals are filtered by a Gaussian filter with a $sigma = 12$. The observations track has been offset by $+17$ mGal and the control track by -32 mGal to control their placement in the plot.
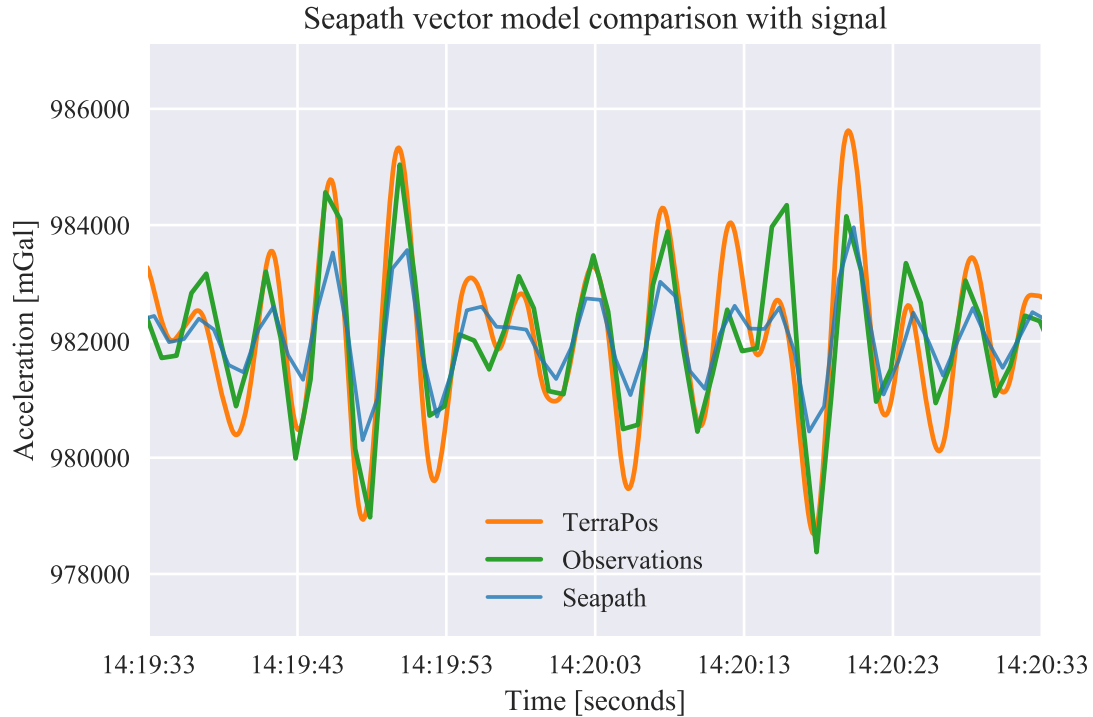
Figure 5.13: A section showing observed signal and calculated model from Seapath and TerraPos data. Notice the difference in amplitude between the models and the observations.

the amplitude of the observations.

Table 5.1 show standard deviations, in $mGal$, for various filter resolutions. The resolution here is calculated from the temporal length of the linear filter used, multiplied by the average speed of the ship. We observe that at lower sampling distances, the seapath method scores as high as the control method does at higher sampling distances. This is in all likelyhood from the reduced amplitude of the spikes during turns. We can see that from figure 5.10 and we can see that in the difference in color value while the ship is turning in figures 5.22 and 5.23

5.5 Correlation

Running the models through a cross correlation with the observed signal from the gravimeter yield some fairly interesting results (Figures 5.14, 5.15, 5.16). We see correlation in all three cases; the control, Seapath and TerraPos methods, but the results from Seapath are so different that they can not be shown in the same plot. This shows that the correlation with the observed signal is on the same order of magnitude for TerraPos and the control method, while it would seem that the correlation with Seapath is three orders of magnitude higher. However, the up - down - up path shown in figure 5.16 raise questions about the models integrity. This will be further discussed in section 6.4.1.

Standard deviation at resolution (units in $mGal$)			
Resolution (GSD)	**Control Δg**	**Seapath δg**	**TerraPos δg**
56m	5.86	4.18	6.04
67m	5.50	3.99	5.80
78m	5.22	3.87	5.66
90m	5.02	3.79	5.56
100m	4.85	3.74	5.49
112m	4.73	3.70	5.43
125m	4.63	3.68	5.38
135m	4.55	3.66	5.35
145m	4.48	3.64	5.32
268m	4.38	3.62	5.27
210m	4.22	3.58	5.20
330m	3.93	3.51	5.07

Table 5.1: An overview of standard deviation in $mGal$ of Δg and δg track results. Resolution is given as ground sample distance (GSD) in meters and corresponds to the approximate length of the linear filter - lower is better

Figure 5.14: Correlation of the TerraPos and the control model with the actual gravitational signal
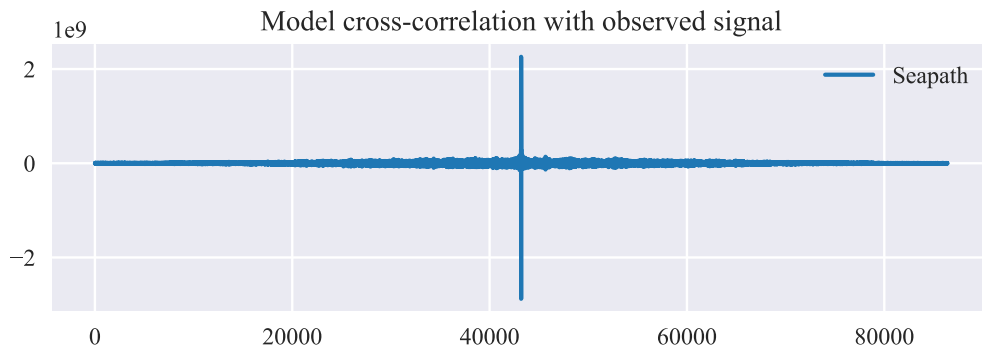
Figure 5.15: Correlation of the Seapath model with the observed signal.
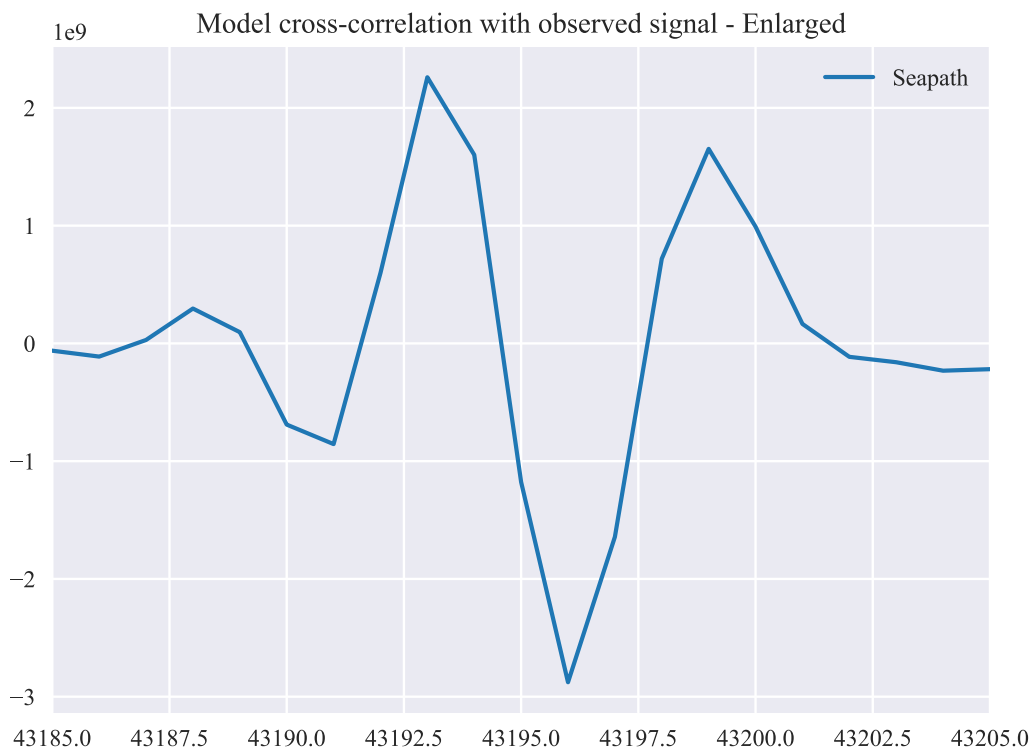
Figure 5.16: A zoomed in view on the peak of correlation between the Seapath model and the observed signal. Notice how the negative correlation is larger than the positive, and how they seem to be offset by exactly three seconds.

5.6 Contributing values

5.6.1 Coriolis effects
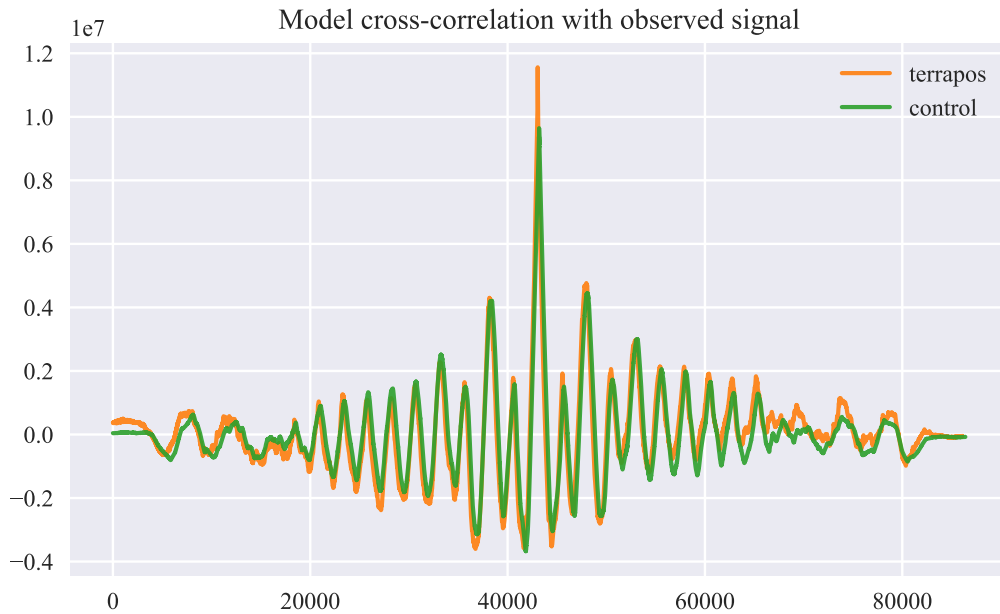
The Coriolis effects in the north and east directions are larger than in the upward direction (the Eötvös effect). In performing scalar corrections these are disregarded, but they should be included when considering vector corrections. However, when the vector equation is collapsed to a scalar value, a square sum is performed. This square sum includes the theoretical gravity γ in the up-down direction, that means the north and east coriolis effets are added perpendicular.

We can show the effect of the horisontal Coriolis components by performing first a square sum of a typical value in the north-east plane, and then perform a square sum with that result and a typical value for γ, and then subtract γ from the result. This would yield the contribution to the total length of the vector:

$$\sqrt{F_{East}^2 + F_{North}^2} = F_{horizontal}$$
$$\sqrt{(30mGal)^2 + (-25mGal)^2} = 39mGal$$
$$\sqrt{F_{horizontal}^2 + \gamma^2} = A$$
$$\sqrt{(39mGal)^2 + 982075^2} = A$$
$$A - \gamma = 0.000774mGal$$

The Eötvös effects are aligned vertically along the same axis as γ so they do not suffer from degredation by the power of the square sum. Eötvös effects calculated from Seapath and TerraPos data do not show any differences other than what appears to be a permanent offset of just over 0.5 mGal (see figure 5.18).

5.6.2 Normal gravity

Considering the difference between equations 2.5 and 2.6, it is no surprise that we observe an offset proportional to ellipsoidal height between γ (calculated for Seapath and TerraPos data) and γ_Q (normal gravity on the ellipsoid), in Figure 5.19. The undulations observed in the Seapath γ but not in TerraPos, are directly proportional to the heights from the Seapath data. However, if we accept the difference between the two γ amount to a fraction of a milligal.

5.6.3 Accelerations

If we consider accelerations in the upward direction with respect to the local-level reference frame and filter them with the RC-filter, we should be left with the contribution that
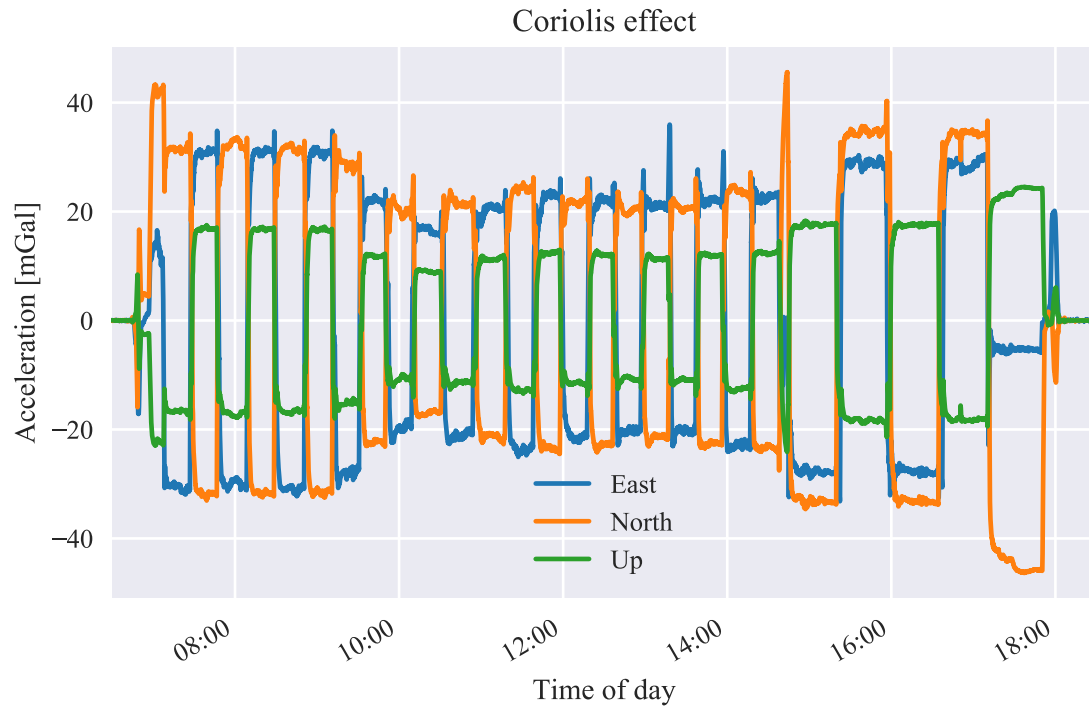
Figure 5.17: Coriolis effects for the duration of the observing mission on March 14th 2016. This plot show Coriolis effects acting in three different spatial dimensions - in one plot.
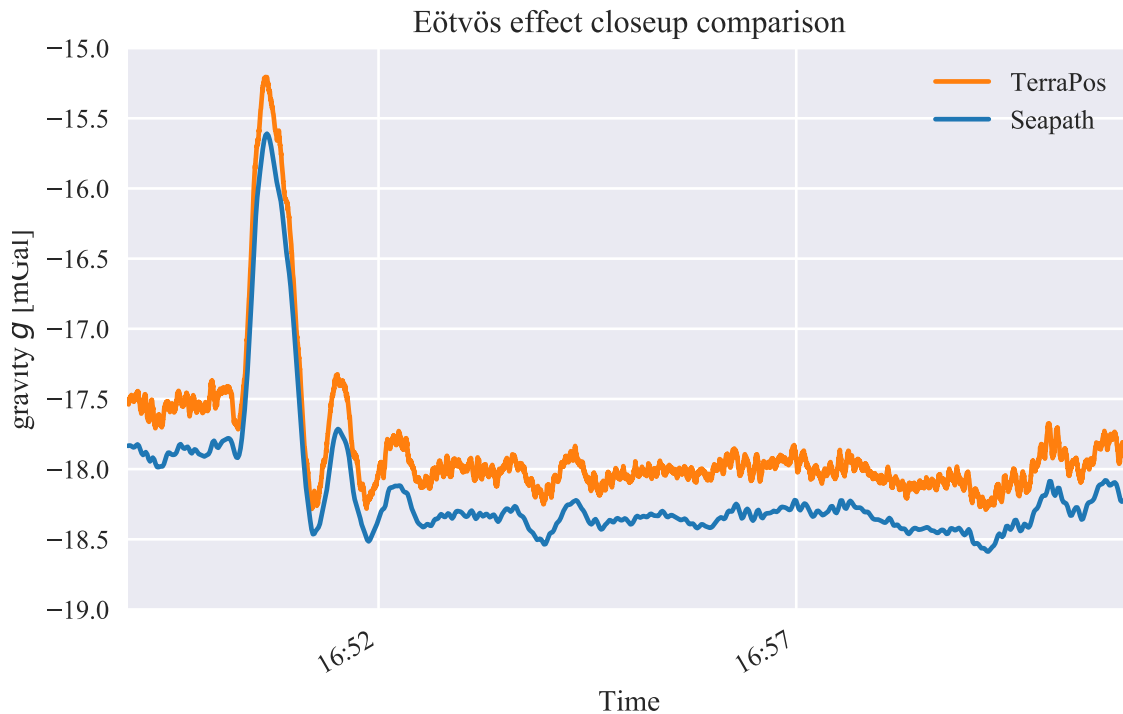
Figure 5.18: Calculated Eötvös effects from Seapath derived velocities and TerraPos exported velocities show a permanent bias offset.
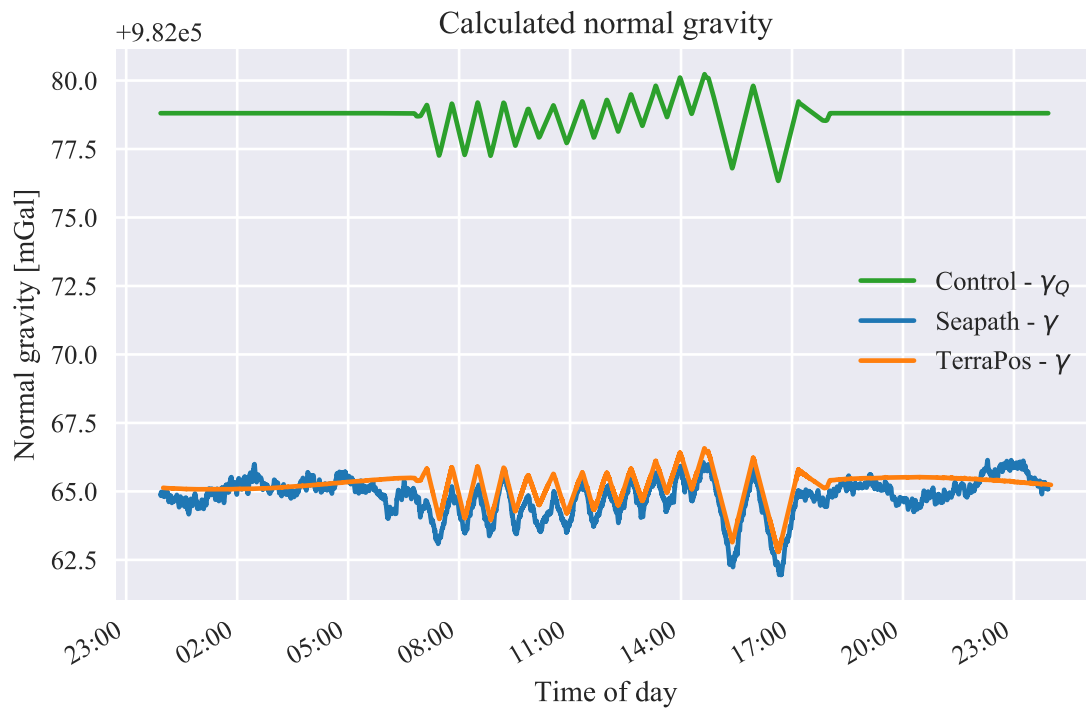
Figure 5.19: Comparison of calculated normal gravity, γ for a point over the ellipsoid and γ_Q on the ellipsoid

the accelerations contribute to the model. In other words, they should be comparable to the raw observations from the gravimeter. Figure 5.20 show a comparison of the two "modelled" accelerations. Observe that the distribution of the Seapath acceleration mimmic that of the gravimeters readout (figure 4.1, while the Terrapos data fluctuate wildly. If the TerraPos accelerations are scaled down by a factor of 10, the variations from when the ship is in dock would be on the same order of magnitude as the seapath data. This is also evident in the northward acceleration comparison shown in figure 5.21 where the accelerations are actually scaled down by a factor of 10 for Seapath.

We see that scaling down by an order of magnitude make the plots look more similar, but this is not implemented in the production of anomalous gravity values because the file header for the TerraPos data in Appendix A explicitly states that accelerations are given in meters per second squared $\left(\frac{m}{s^2}\right)$.

44
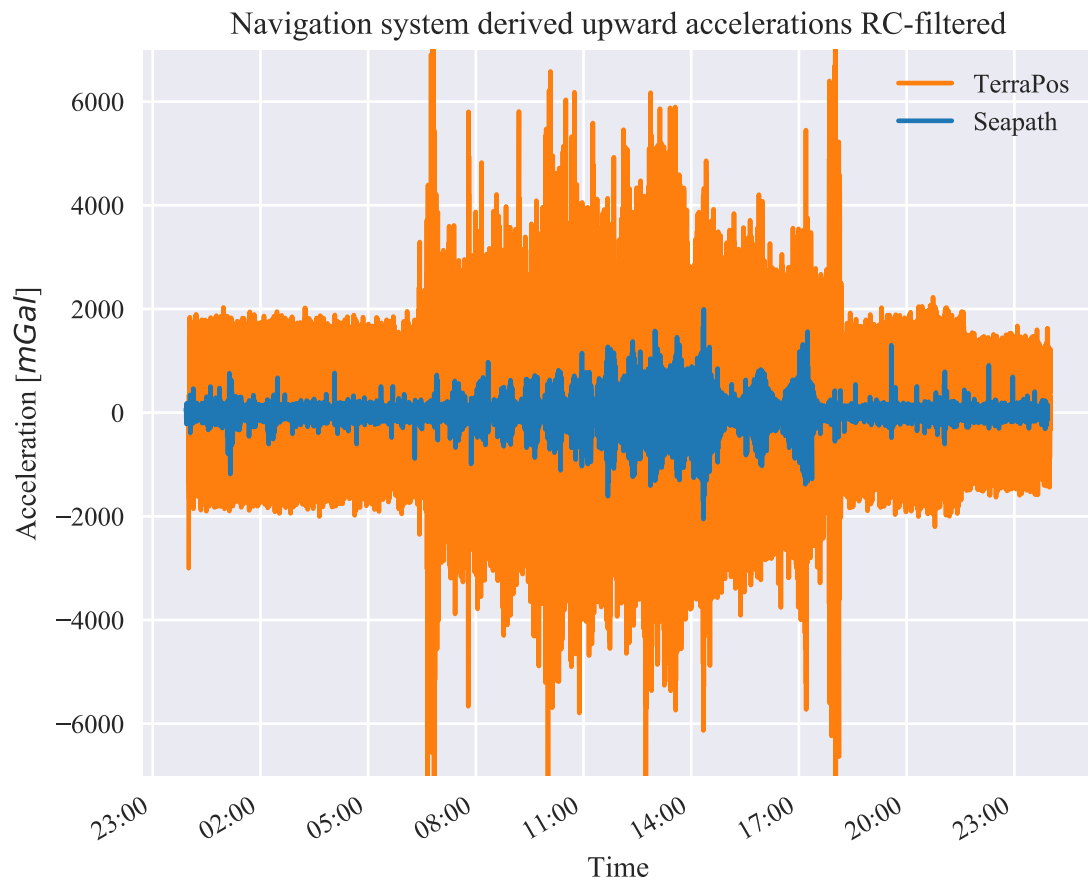
Figure 5.20: Accelerations in the upward direction from TerraPos and Seapath data filtered with an RC-Filter with $RC = \tau = 4.5s$
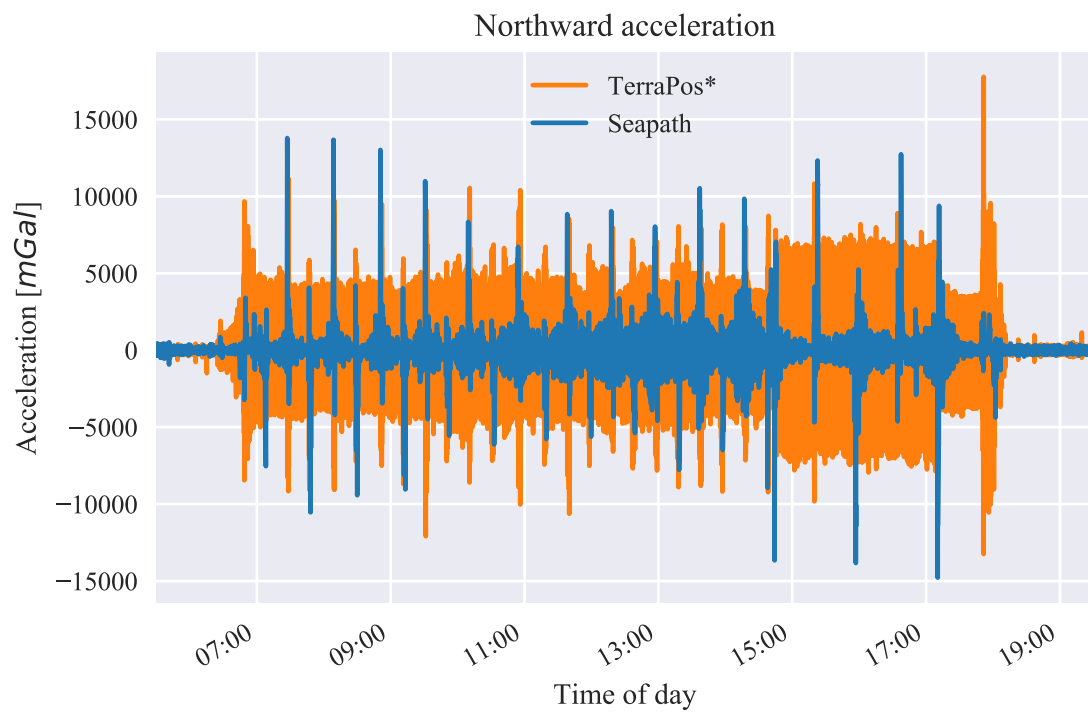
Figure 5.21: Northward accelerations. * TerraPos accelerations are scaled down by a factor of 10!
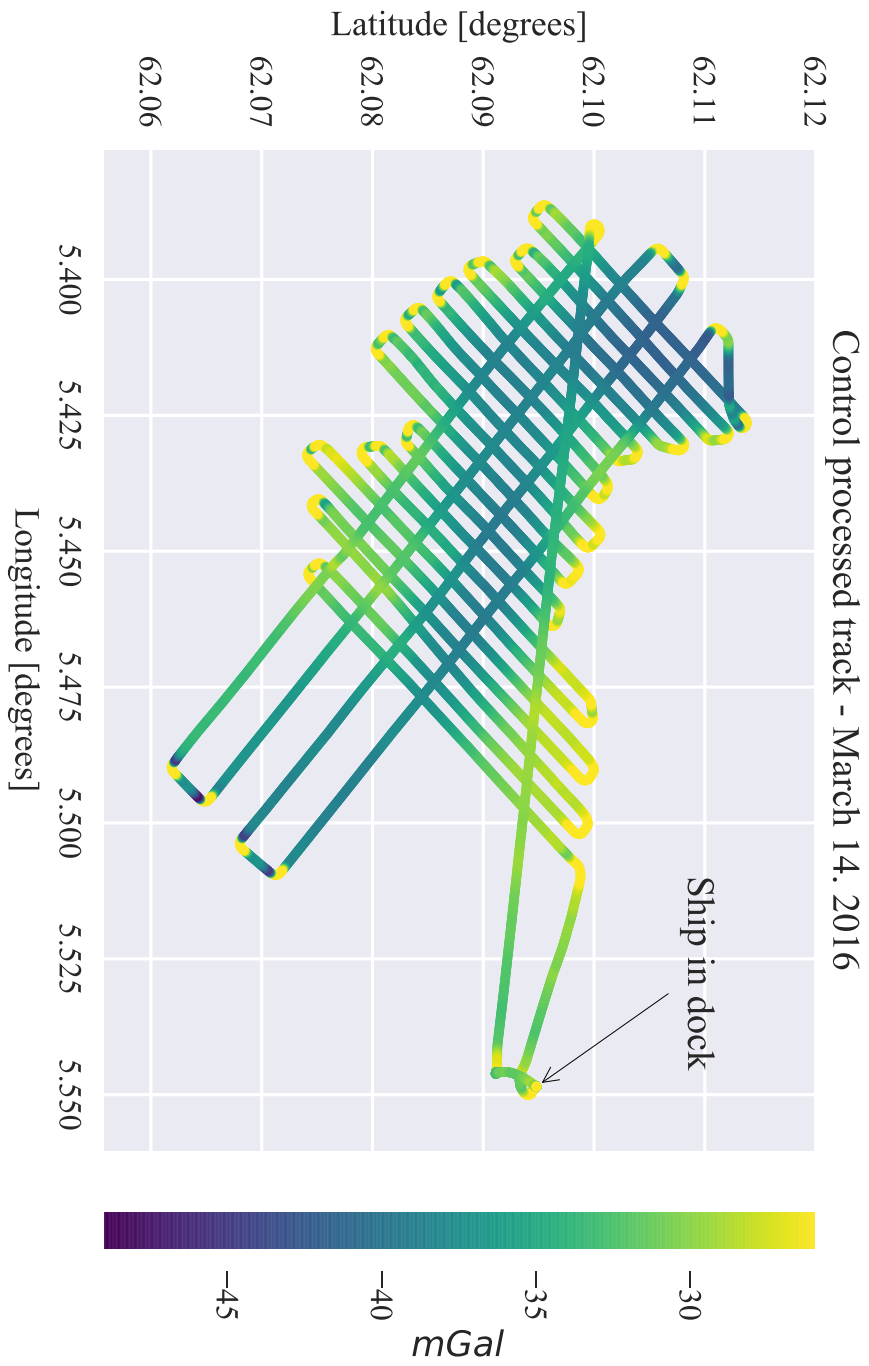
Figure 5.22: A track showing the application of the control method.
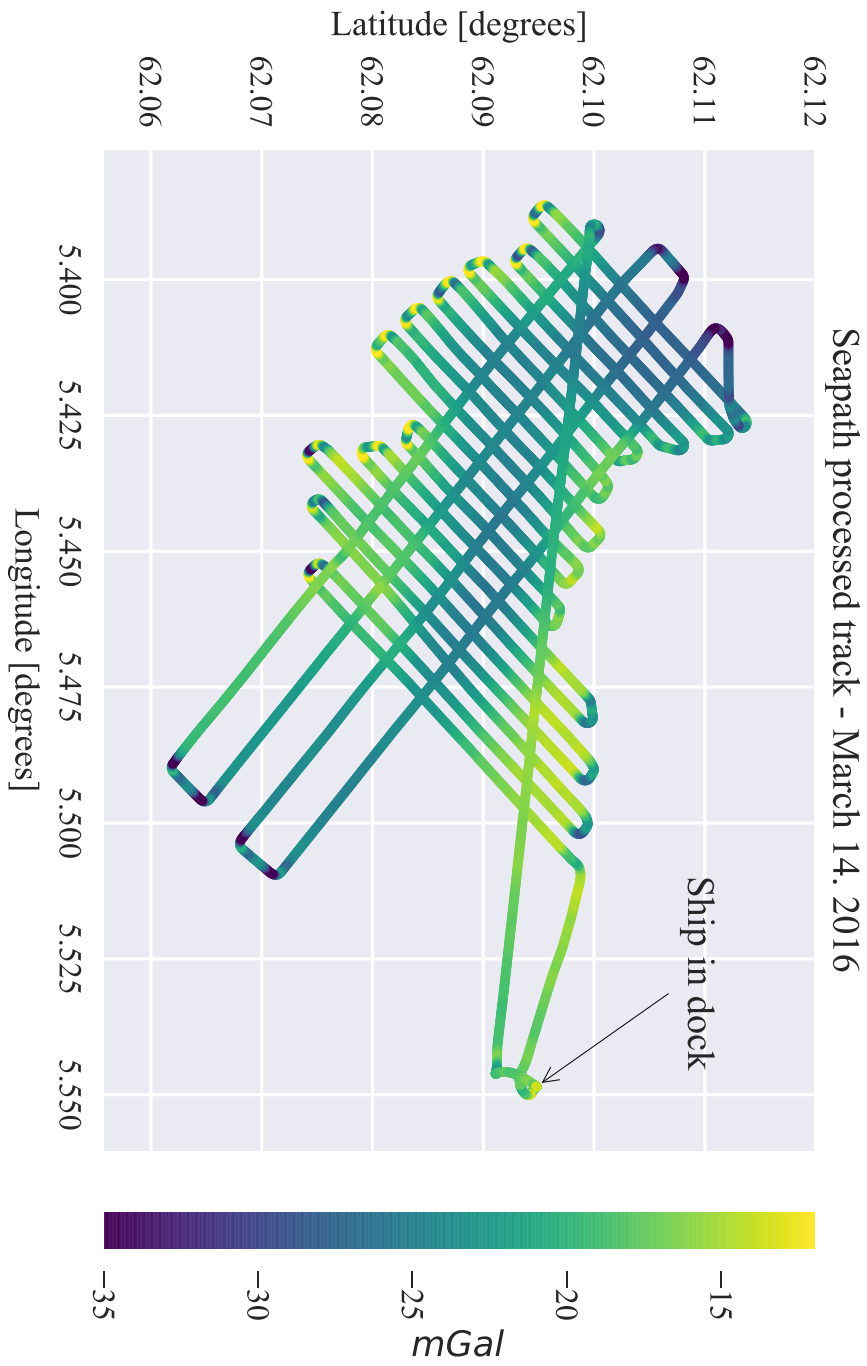
Figure 5.23: A track showing the application of the Seapath method.
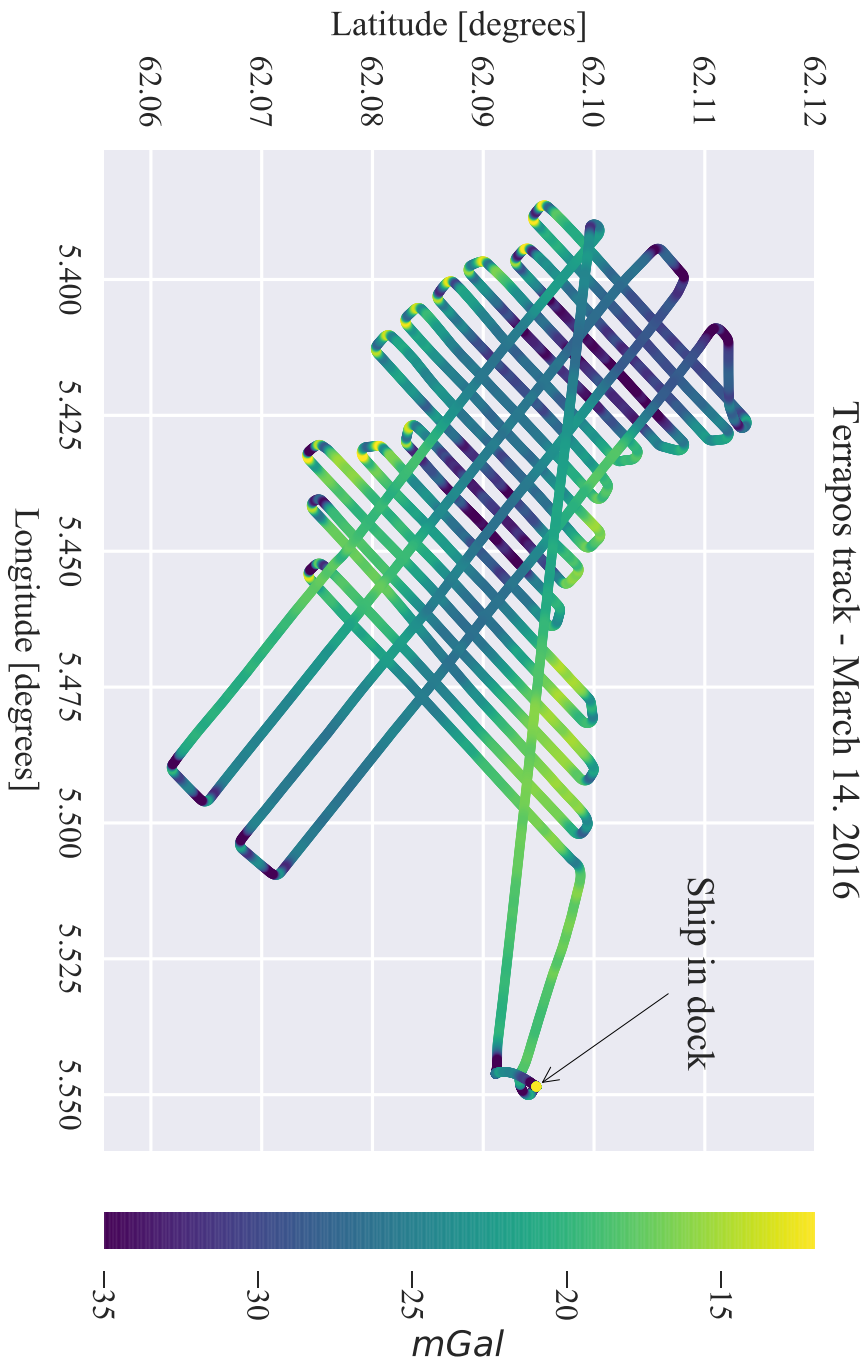
Figure 5.24: A track showing the application of the TerraPos method.

Chapter 6

Discussion

The BGM-3 gravimeter is designed to be always-on. This means that it will continue to record the state of acceleration acting on the test mass as long as the platform (ship) or its battery backup can supply it with power. This thesis makes two assumptions of the measuring instrument: That it is working as intended, and that it has not been turned off intentionally or otherwise to disrupt its current calibration.

6.1   Development

During practical development of the TerraPos method, it became apparent that the important parameters from the TerraPos post process operation were: GPS time, position (including ellipsoidal height), velocity, and acceleration in the local ENU reference frame. TerraPos has the ability to export many different parameters in any given reference frame. Initially, the exports, i.e. the available data consisted of parameters in the Ships reference frame. This added a layer of complexity since velocity and accelerations had to be rotated to ENU manually. Simply having ENU velocities, for example, simplified the programming approach of finding the Eötvös effect, and similarly, made ship acceleration more intuitive to understand.

6.2   On accelerations

According to the Nyquist sampling theorem (Genrich and Minster (1991)), a signal needs to be sampled at two times the frequency to correctly determine the signal. In this case, it both works for and against our developed methods: In one way, we are sampling at a higher frequency than ocean surface waves that we wish to estimate. Ocean surface waves can have frequencies stretching from 0.5 Hz to 0.05Hz (Geos, 2001). But on the other hand, we are trying to estimate the signal from the gravimeter with an output of 1 Hz. We should be sampling position at 2 Hz.

This frequency distribution of ocean waves is also the foundation for the choice of limiting the upward accelerations with a high pass filter of 0.08 Hz. Horizontal accelerations were low-pass filtered with a cut-off frequency of 0.1 Hz. This choice was more empirical than theoretical since it was determined by trial and error: The gyro-stabilised platform will maintain verticality in the case of a horizontal jerk[1], but for sustained accelerations, it will slowly drift towards the total acceleration vector by some time constant. What this time constant is, is yet to be determined.

Figure 5.12 clearly shows that our models and the observed signal follow each other tightly. The models have undergone RC-filter discussed in section 2.4.1 (implementation can be found in Appendix B), to estimate the output of the gravimeter. In the development process, this was a significant milestone because it provided intuitive evidence that the method had merit.

At this time we are well within the limits of measurement physics: The particulars of the gravimeter and its stabilising platform transcends the bounds of physical geodesy. The correct estimation of acceleration in the vertical direction is paramount to the success of these methods, and figure 5.12 show that we are on the right track. In fact, from that graph, it looks like the TerraPos model might be better. But the correlation results (figure 5.16, show a strong negative correlation. This indicates that there might be something wrong in how accelerations are handled, and the running theory is that accelerations in the Seapath model are offset by three seconds and added to the vertical component with the wrong sign.

6.2.1 Prefiltering of position

In some cases, it would be wise to implement a Kalman filter or Least squares fitting to some of the raw data. For instance, positional measurements by the Seapath system often have a quantised or step-like profile. Either, this is due to the accuracy of the measurements, or the numerical limitations of the NMEA sentences sent to the recording computer. It was essential to resolve this step-like profile into something that would more accurately reflect the natural motion of this massive ship. However, implementing an optimal solution like a Kalman filter was impractical, and since TerraPos is supposed to use Kalman filtering, it was decided to approach the Seapath data differently. The solution is to apply a Gaussian convolution filter to the data, effectively smoothing out the step-like artefacts. Height above the ellipsoid was the noisiest and required strong Gaussian filtering. The result of this was that the first and second derivatives were not plagued by the blocking artefacts. This is essentially a fitting, meaning that a false or inaccurate measurement affect the track to the same degree as a good measurement.

---

[1]From physics, jerk is the name for the derivative of acceleration with respect to time.

6.3   Vector considerations

One of the fundamental reason why the vector models were developed was because of a lack of a readout on the x-y accelerometer in the stabilised platform subsystem of the BMG-3. These measured accelerations could be used to perform a correction, as they contain information about the orientation of the platform. Peters and Brozena (1995) discuss methods for using GPS derived acceleration instead of these measurements. However, their approach is centred around finding the deflection angle of the platform subsystem. A direct approach using their methods might be useful to investigate.

The TerraPos method is, in essence, the same as the Seapath method, with one important caveat. The derived acceleration and velocity vectors are computed by TerraPOS at a rate of 10Hz compared to the 1Hz real-time solution provided by Seapath. As such, we would expect the results from TerraPOS to be of higher and more consistent quality. However, that is not what the results show. Only when looking at the individual components like height and velocity by themselves, can we see that TerraPos data are more accurate.

6.4   Main findings

From the results we see conclusive evidence that there is correlation between our models and the observed signal (figures 5.14 and 5.15) and we find intuitive evidence of the same in figure 5.12.

We have found that the main difference between scalar and vector considerations applied to the Seapath data is the estimation of turning spikes also seen in the observations (figure 5.12).

We see that filtering applied in the result section suppress high frequencies (all plots showing power spectral densities, i.e. Figure 5.11). However, we do not see a significantly better result from the Seapath method than we see for the control method across the track (figure 5.12.

6.4.1   Correlations

The correlation plot showing the negative correlation between the Seapath method and the observed signal (figure 5.16) may indicate that something is wrong with the Seapath model, as discussed above, which warrants further investigations. It may be that this fault is why so much filtering is needed to get a comparable result with the control model. And why the standard deviations in table 5.1 are not better for the Seapath data.

The TerraPos model does not show the same negative correlation. It has a positive spike only and is on the same order of magnitude as the control method. Considering the difference between the Control- and TerraPos model shown in figure 5.12 we see that they

are very different in regards to high frequency variations (of which the control model has none) and yet they correlate at the same order of magnitude.

6.4.2 Deductions

Having reduced the spikes from the centrifugal effects of turning, a long duration filter would not be so much affected by the spikes as before. This means that reducing the spiking would make more of the ends of each track usable in gravimetric calculations. Furthermore, if the spikes can be removed entirely, this opens up the possibility of not trimming away the turns when using the data. For instance, a non-linear filter can be designed to apply a low weight to data captured while the ship is turning.

6.5 Future work

Going forward, here are a few recommendations of future work in no particular order:

- The results should be validated by calculating the crossover RMS. We can get an intuitive understanding of how well each crossover point is related to the one below by studying the three maps at the end of the result section.

- The amplitude difference between the observations and the models should be investigated.

- The method put forth by Peters and Brozena (1995) to calculate the deflection angle of the platform should be investigated as a substitute for adding the horizontal accelerations directly.

- A better method for defining resolution should be implemented. The methods discussed here assumes the spatial resolution is equal to the length of the final filter. The effects of a linear convolution kernel applied after a Gaussian convolution kernel may have little effect on the signal unless the linear convolution kernel is significantly longer.

- Develop a simple Kalman filter for the Seapath data

- Calculate acceleration by the second derivative of the positions provided by the TerraPos, to confirm whether or not the exported accelerations are faulty.

6.6 Notes

In working on this thesis, we have encountered a few items of interest that may be worthy of note.

Computation time   In the greater scheme of things, computational time of this data is negligible. It takes only seconds to compile the python code, load the raw data and run the entire process. Some optimisation has already been made to cut down testing time in development. It is recommended that data handling is not done with for-loops as to not increase computational time unnecessarily.

Database integration   Designing the methods with the use of Pandas should allow for easier integration with database systems. It may be useful to migrate the current stock of raw data logs from a file system to a more comprehensive database.

Resampling and comparison   It may be useful to super-sample and smooth both model and observation to compare them graphically or with a correlation function. Resampling the model to the observation times of the gravimeter turned out to be a good idea. But if we up-sample the positions in the Seapath (for instance with a Kalman filter), we may be able to define a time offset to resample the signal to more accurately.

Fuel tank contribution   Rumors about gravimetric time series being ruined by construction due to additional mass being added nearby, prompted an investigation into the ships fuel tanks. Observing the relative position of the gravimeter and a $42m^3$ fuel tank 4 meters directly underneath, a back of the envelope calculation reveled that:

$$a = G\frac{42000l \times 0.832kg/l}{(4m)^2}$$

$$a = 1.46 \times 10^{-7}\frac{m}{s^2} = 0.0146mGal$$

Q.e.d. The contribution is significantly less than the noise floor of the gravimeter and thus did not warrant further investigations. This would be significant if the gravimeter had an accuracy comparable to that of an absolute gravimeter.

5 mGal   There is a measurement uncertainty of 5 mGal in each sample of the gravimeter's data: Since the Counter Units are all integer from the embedded analog-to-digital converted(ADC), and the scale factor from counter units to milligal is 4.911302. This error propagates to the final product and may be the reason why we cannot get more accurate data than 1 mGal / 0.1 km. If the model correctly estimates *each point* of the observed signal (except from *deltag*) we would still expect residuals from this quantization.

Chapter 7

Conclusion

The corrective vector model from Seapath data shows that GNSS derived accelerations can be used in correcting BGM-3 gravimetry data. However, the results were worse than expected: Compensating for acceleration does not seem to significantly improve the results along track since the result is noisy and require a large amount of filtering. The filtering required to eliminate this noise is such that it nullifies the effects of compensating for the accelerations. The horizontal accelerations, resulting from big turns, are longer in duration and therefore escapes the effects of filtering enough to affect the results positively. We have proved that horizontal accelerations can be used to reduce artefacts from these turns without knowing the orientation of the gravimeter as it rests on a stabilised platform. However, lowering the faulty contributions from turns allows a long duration filter to be applied without negative impacts affecting gravimetric observations at the start and end of each line. We can speculate that using wide, round turns instead of two-point turns would alleviate peaking and allow for better estimation of horizontal accelerations.

These investigations conclude that the Seapath data are of a sufficient quality to be used to model inertial effects in the observing platform. However, we recommend the use of a simple Kalman filter to reduce high-frequency noise from inaccuracies of positions and from quantisation due to rounding. Accelerations exported from TerraPos (in our case) are noisy and should not be used. Investigations should be made about the viability of TerraPos positions and their derivatives outside TerraPos, to establish if the problem is confined to accelerations.

Ultimately the measure of standard deviations across the entirety of the track is a poor indicator of quality. However, the lower standard deviations from the Seapath method is evidence that the vector considerations had a positive impact in relation to the objective. The spikes resulting from turning have been successfully suppressed, even though we have no conclusive evidence that it affects the crossover RMS.

Bibliography

Bell (1979). Operation and maintenance manual for gravity sensor subsystem BGM-3. Technical report, Bell Aerospace Textron, Buffalo.

Bell (1987). Operation and maintenance manual for the BGM-3 stabelized platform subsystem. Technical report, Bell Aerospace Textron, Buffalo.

Bell, R. E. and Watts, A. B. (1986). Evaluation of the BGM-3 sea gravity meter system onboard R/V Conrad. *Geophysics*, 51(7):1480–1493.

Bratheim, P. C. (2017). Felles referanseramme for sjø og land på Søre Sunnmøre fase 1. Technical report, Kartverket.

Einstein, A. (1915). On the general theory of relativity. *Sitzungsber. Preuss. Akad. Wiss. Berlin (Math. Phys.)*, 1915:799–801.

Genrich, J. F. and Minster, J.-B. (1991). Near-real time reduction of shipboard gravity using Kalman-filtered GPS measurements. *Geophysics*, 56(12):1971–1979.

Geos, F. (2001). *Wind and wave frequency distributions for sites around the British Isles.* Great Britain, Health and Safety Executive.

Harlan, R. B. (1968). Eotvos corrections for airborne gravimetry. *Journal of Geophysical Research*, 73(14):4675–4679.

Haugen, F. (2008). Derivation of a Discrete-Time Lowpass Filter. *Differentiation*.

Hofmann-Wellenhof, B. and Moritz, H. (2006). *Physical geodesy.* Springer, 2nd, corr. edition.

Jones, E., Oliphant, T., Peterson, P., et al. (2001–). SciPy: Open source scientific tools for Python. [Online; accessed May 14, 2018].

Kalman, R. E. (1960). A new approach to linear filtering and prediction problems. *Transactions of the ASME–Journal of Basic Engineering*, 82(Series D):35–45.

McKinney, W. (2010). Data structures for statistical computing in python. In van der Walt, S. and Millman, J., editors, *Proceedings of the 9th Python in Science Conference*, pages 51 – 56.

Neumeyer, J., Schäfer, U., Kremer, J., Pflug, H., and Xu, G. (2009). Derivation of gravity anomalies from airborne gravimeter and IMU recordings-Validation with regional analytic models using ground and satellite gravity data. *Journal of Geodynamics*, 47(4):191–200.

Omang, O. C. D. (2017). Base reading - Gravity tie - Hydrograf. Technical report, Kartverket, Oslo.

Peters, M. F. and Brozena, J. M. (1995). Methods to Improve Existing Shipboard Gravimeters for Airborne Gravimetry. In *Proceedings of the IAG Symposium on Airborne Gravity Feild Determination*, pages 39–46, Boulder, Colorado, USA.

Pérez, F. and Granger, B. E. (2007). Ipython: A system for interactive scientific computing. *Computing in Science & Engineering*, 9(3):21–29.

Scargle, J. D. (1982). Studies in astronomical time series analysis. II - Statistical aspects of spectral analysis of unevenly spaced data. *The Astrophysical Journal*, 263:835.

Torge, W. and Müller, J. (2012). *Geodesy*. Walter de Gruyter.

Wei, M. and Schwarz, K. P. (1995). Analysis of GPS-derived acceleration from airborne tests. In *International Association of Geodesy Symposium G*, volume 4.

Appendix A

TerraPos output header

```
Output from TerraPos

TerraPOS version 2.4.2 (5358cb0), system files version: 2018-02-09


Reference frame in navigation file:
ITRF2008(2016.19983)
Gravity model: GRS80 normal gravity

Ellipsoid: GRS80 (a=6378137.0000, f=1/298.25722210)


 Output refers to: gravimeter
Platform to output cardinal rot.:R1= 0.00 deg, R2= 0.00 deg, R3= 0.00 deg
Boresight angles (p-frame):      R1= 0.00 deg, R2= 0.00 deg, R3= 0.00 deg
Platform to output lever-arm:    dx=-2.07 m,   dy=-1.44 m,   dz= 0.97 m#

INS, Tightly coupled
Output:
ISO date/time spec: %Y-%m-%dT%H:%M:%s (GPS)
Latitude (Degrees)
Longitude (Degrees)
Ellipsoidal height (m)
E-vel
N-vel
U-vel
East acceleration (m/s2)
North acceleration (m/s2)
Up acceleration (m/s2)
R1 (g-frame to platform frame), unit deg, Rot. seq. XYZ_S, -180 - 180 deg
R2 (g-frame to platform frame), unit deg, Rot. seq. XYZ_S, -180 - 180 deg
R3 (g-frame to platform frame), unit deg, Rot. seq. XYZ_S, -180 - 180 deg
```

Appendix B

Data processing functions

```python
def RC_filter(timeseries, dt=0.1, RC=4.5):
    """Descrete time lowpass filter
    derived from backward differentiation approximation
    ref. Derivation of a Discrete-Time Lowpass Filter by Finn Haugen

    Magne Bugten 2018-04-12

    This function simulates the output across an RC filter with a time
    constant "RC" given in seconds. It is an approximation, and
    according to Finn Haugen, it will hold true as long as dt < (RC/5),
    which it is, given the initial conditions, but would not be for 1Hz
    data!

    Args:
        timeseries: Input values of the function; that which is to be
        filtered [arraylike]
        dt: timestep in seconds, defaults to 0.1
        RC: time constant of filter in seconds, defaults to 4.5

    Returns:
        out: filter response, arraylike. """
    a = dt/(RC+dt)
    out = np.zeros(timeseries.shape[0])
    prev=timeseries[0]
    for index, value in enumerate(timeseries):
        out[index] = (1-a)*prev + a*value
        prev = out[index]
    return out


def gauss_filter(data, length=30, sigma=5):
    """Filters position data with a padded gausian filter"""
```

```python
        # Padd the data so endpoints are not all wack
        dat = np.pad(np.asarray(data), length, mode='edge')

        # Define Gaussian window
        window = signal.gaussian(length, std=sigma)

        # Perform convolution with Gaussian window + devide by sum of
        # the window
        out = signal.convolve(dat, window, mode='same') /sum(window)

        # remember to remove padding on output
        return out[length:-length]


def linear_convolve(data, s=1.0, dt=0.1):
    window_length = int((1.0*s)/dt) + 1
    window = [1/window_length]*window_length

    # Padd the data so endpoints are not all wack
    dat = np.pad(np.asarray(data), window_length, mode='edge')

    # Perform convolution with Linear window
    out = np.convolve(dat, window, mode='same')

    # remember to remove padding on output
    return out[window_length:-window_length]


def butter_filter(data, cutoff, fs, order=5, btype='low'):
    nyq = 0.5 * fs
    # desired cutoff frequency of the filter, Hz
    normal_cutoff = np.float(cutoff) / nyq
    b, a = butter(order, normal_cutoff, btype=btype, analog=False)
    y = lfilter(b, a, data)
    return y

def normal_gravity(lat, height):
    """Estimates the normal gravity for GRS80 for an array
    Origional by Ove Omang
    modified by Magne Bugten 2018-03-12
    Args:
            lat: degrees of latitude [array-like]
            height: ellipsoidal height [array-like]
    Returns: [mGal]
            grav80: Normal gravity for all points in input arrays
    >>> normal_gravity(54.32300000,1.8)
```

```python
    981448.97475"""

    latitude=lat
    gamma_e=978032.67715
    sin2 = np.sin(np.radians(latitude)) * np.sin(np.radians(latitude))
    gamma_expansion = ( ( (  7.0*np.power(10.0,-10 )*sin2 +
                            1.262*np.power(10.0,-7) )*sin2 +
                          2.32718*np.power(10.0,-5) )*sin2 +
                       5.2790414*np.power(10.0,-3) )*sin2 + 1.0

    fa = (7.2651*np.power(10.0,-8)*height +
         4.38983*np.power(10.0,-4)*sin2 -
         0.308779814)*height

    grav80 = fa + gamma_e*gamma_expansion
    return grav80


def coriolis_effect(lat, e, n, u, deg=True):
    """Estimates coriolis for all ENU vector component
    including centrifugal effects
    Args:        [array-like]
         lat: geodetic latitude
         e: Eastward velocity [m/s]
         n: Northward velocity [m/s]
         u: Upward velocity [m/s]
         deg=True: false if lat is given in radians
    Returns:         [units in mGal]
         aeast: Eastward coriolis vector
         anorth: Northward coriolis vector
         eot: Eotvos effect upward """
    if deg:
        lat = np.radians(lat)
    OMEGA = 7.2921150e-05 #radii per sec
    R = 3671000.0 #meters
    sinlat = np.sin(lat)
    coslat = np.cos(lat)
    aeast = (2*OMEGA*(n*sinlat - u*coslat))*1e+05
    anorth = (-2*OMEGA*e*sinlat)*1e+05
    aup = (2*OMEGA*e*coslat)*1e+05
    # The second term in the Eötvös effect reflects the
    # centrifugal force needed to stay on the sphere.
    centrifugal = ((np.power(e,2) + np.power(n,2))/R)*1e+05
    eot = aup + centrifugal
    return aeast, anorth, eot
```

```python
def free_air(H):
    """Calculate free air reduction
    H: height to be reduced
    return:"""
    return 0.3086*H # [mGal]


def CV_adjustment(CV, base_counter, base_gravity, reduction_height,
                  scale_factor=4.911302):
    """Calculate measurements from rawdata and reference point.
    Assumes a linear scale factor for the gravimeter
    ARGS:
        CV: List containing Counter Values. Array-like
        base_counter: relative gravimeter reference value at t0
        base_gravity: Gravimetric calibration point value at t0
        reduction_height: height of base_gravity over g0
    Return:
        g_measurement: unumpy array containing direct measurement
        of g in mGal"""
    # Perform the free air reduction by adding height*gradient to
    # observed point. If "reduction_height" is zero there will be
    # no reduction.
    g0 = base_gravity + free_air(reduction_height)
    reading = (CV - base_counter)*scale_factor
    return g0 + reading


def linear_drift(t_obs, t_ref, drift_rate=0.066):
    """Compute drift values to be added to measurememnts
    Args:
        t_obs: Observation times, array of datetime objects
        t_ref: Datetime object refferring to time of calibration.
        drift_rate=0.066: 0.066 by default, daily drift ratein mgal.
    Returns:
        drift: array of offset values in mGal.  """
    drift_sec = drift_rate/24/3600
    return [(time-t_ref).total_seconds()*drift_sec for time in t_obs]


def reindex_and_interpolate(old_index, new_index=pd.DataFrame()):
    """Interpolate values in one dataframe for timestamp in a second.
    Args:
        old_index: Dataframe to be converted
        new_index: Optional, Dataframe, source of the new index
                    If not given or empty df, interpolation starts
                    on the next full second with 1s intervals.
    Returns:
```

```python
        out: new interpolated dataframe """
    if new_index.empty:
        new_index = \
        old_index.reindex(old_index.resample('1s',closed='right')\
                                    .asfreq('1s').index,
                                    method=None).reset_index()
    new_index = new_index[['GPS_time']].copy()
    old_index = old_index.reset_index()

    # Join the two arrays
    result = pd.concat([old_index, new_index]).sort_values('GPS_time')\
                    .reset_index(drop=True)

    # Set index to GPS_time in the resulting dataframe
    result.set_index('GPS_time', inplace=True)
    result.to_csv('Data/look_here.csv')

    # Interpolate, using pandas interpolate that calls scipy's interp1d
    kwargs={'fill_value':'extrapolate'}
    result = result.interpolate(method='cubic', **kwargs)

    # Extract correct times
    out = result.loc[new_index.GPS_time].reset_index()\
                                    .set_index('GPS_time')
    return out


def differentiate(X):
    """Differentiates dataframe X
    Differentiation removes one endpoint in array!"""
    dx = pd.DataFrame((X[2:].values - X[:-2].values)/2.0,
                    index=X.index[1:-1], columns=X.columns)
    return dx


def double_diff(X):
    """Double differentiate X dataframe
    Differentiation removes one endpoint in array!"""
    ddx = pd.DataFrame(X[2:].values - 2*X[1:-1].values + X[:-2].values,
                    index=X.index[1:-1], columns=X.columns)
    return ddx


def df_geodetic2ecef(df, ell=None, deg=True):
    """Run the geodetic2ecef function from pymap3d for a
    dataframe containing  lat, lon, h, with optional arguments."""
    if not df.index.name == 'GPS_time':
```

```python
        df.set_index('GPS_time')

    x,y,z = pm.geodetic2ecef(np.asarray(df.lat),
                             np.asarray(df.lon),
                             np.asarray(df.h),
                             ell=ell, deg=deg)

    cols = [['X', 'Y', 'Z']]
    out = pd.DataFrame(data=np.stack((x,y,z), axis=1),
                       index=df.index, columns=cols)

    return out


def df_ecef2ned(vector, location, deg=True):
    """Pandas wrapper for pymap3d.ecef2med
    Args:
        vector: df with vector to transform
        location: dataframe containing lat, lon coordinates
    Returns:
        out: dataframe with corresponding vector"""
    location = location.loc[vector.index]
    e, n, u = pm.ecef2enuv(vector.X.values.flatten(),
                           vector.Y.values.flatten(),
                           vector.Z.values.flatten(),
                           location.lat.values.flatten(),
                           location.lon.values.flatten(),
                           deg=deg)
    cols = ['E', 'N', 'U']
    out = pd.DataFrame(data=np.stack((e,n,u), axis=1),
                       index=vector.index, columns=cols)
    return out
```